

APPLICATION OF COSMO-RS IN GAS HYDRATE MITIGATION

LIEW CHIN SENG

CHEMICAL ENGINEERING
UNIVERSITI TEKNOLOGI PETRONAS
SEPTEMBER 2015

Application of COSMO-RS in Gas Hydrate Mitigation

by

Liew Chin Seng

15247

Dissertation submitted in partial fulfilment of
the requirements for the
Bachelor of Engineering (Hons)
(Chemical Engineering)

SEPTEMBER 2015

Universiti Teknologi PETRONAS
32610, Bandar Seri Iskandar,
Perak

CERTIFICATION OF APPROVAL

Application of COSMO-RS in Gas Hydrate Mitigation

by

Liew Chin Seng

15247

A project dissertation submitted to the
Chemical Engineering Programme
Universiti Teknologi PETRONAS
in partial fulfilment of the requirement for the
BACHELOR OF ENGINEERING (Hons)
(CHEMICAL ENGINEERING)

Approved by,

(Dr Bhajan Lal)

UNIVERSITI TEKNOLOGI PETRONAS
BANDAR SERI ISKANDAR, PERAK
September 2015

CERTIFICATION OF ORIGINALITY

This is to certify that I am responsible for the work submitted in this project, that the original work is my own except as specified in the references and acknowledgements, and that the original work contained herein have not been undertaken or done by unspecified sources or persons.

LIEW CHIN SENG

ABSTRACT

Formation of gas hydrate in oil and gas pipelines has resulted in flow assurance problem. Ionic liquid (IL), due to its dual functionality has been considered as a very promising hydrate inhibitors. However, experimental testing of IL alone is insufficient to examine all potential ILs combinations due to high number of cation and anion to form ILs. Therefore, in order to screen potential ILs prior to narrow down the amount of potential ILs for experimental work, it is helpful to have a predictive model that could satisfactorily pre-screen ILs or to validate experimental work just by considering the fundamental properties.

In this context, four fundamental properties of IL-hydrate system namely sigma profile, hydrogen bonding energies, activity coefficient, and solubility were stimulated through Conductor-Like Screening Model for Real Solvent (COSMO-RS). They were then analyzed to determine if they could be correlated with IL inhibition ability. Among them, sigma profile and hydrogen bonding energies, which later upgraded to total interaction energies exhibit significant relationship with IL inhibition ability. Sigma profile graph in general gives a qualitative understanding in whether certain IL is hydrophobic or hydrophilic. Total interaction energies of ions, on the other hand, have successfully been applied to develop a model that could predict IL thermodynamic inhibition ability in terms of average temperature depression. The correlation was validated with experimental values from literature with an average error of 20.49%. Findings also suggest that this correlation is not suitable to be used for substituted cations, due to the extra H-bonding provided by substituted functional group such as hydroxyl group. Finally, through the use of sigma profile graph and developed correlation, the inhibition ability of 20 ammonium based ILs have been predicted. TMA-OH, due to its short alkyl chain length cation and highly electronegative anion has shown the most promising inhibition ability among 20 of them. It is predicted to be able to depress temperature of IL-hydrate system by 1.97°C, whereas the widely studied EMIM-Cl can only experimentally depress the system by 1.22°C.

ACKNOWLEDGEMENT

First of all, I would like to express my heartfelt gratitude towards my respected supervisor, Dr Bhajan, who gave me guidance and advice to complete this project. Next, I would also acknowledge my sincere appreciation to Dr Kiki, who had assisted and supported me a lot in understanding and working with COSMO-RS. The project could not have been successful without his help. Not to forget is another huge thank you dedicated to Mr Saad, a PhD student that had assisted me in many ways too. The knowledge and advice that he shared had enabled me to complete this project smoothly.

Special thanks to all examiners that have assessed me since the very first Proposal Defence and Pre-SEDEX presentation. The feedback provided has definitely allowed me to further improve my project. Furthermore, a big gratitude goes to our coordinator, Dr Nurul Ekmi for her continuous monitoring and supporting of the FYPII project.

Last but not least, I would like to credit all my achievements in this project to my parents for their never ending support and guiding. Without their encouragement, I could not have been here today. Again, I would like to say thank you to all my friends, colleagues and to those who has assisted me directly or indirectly in completing this project.

TABLE OF CONTENTS

CERTIFICATION OF APPROVAL	ii
CERTIFICATION OF ORIGINALITY	iii
ABSTRACT	iv
ACKNOWLEDGEMENT	v
CHAPTER 1: INTRODUCTION	1
1.1 Background of Study.....	1
1.2 Problem Statement	3
1.3 Objectives.....	4
1.4 Scope of Study	4
CHAPTER 2: LITERATURE REVIEW AND THEORY.....	5
2.1 Ionic Liquids as Gas Hydrate Inhibitor	5
2.2 COSMO-RS	7
2.2.1 Sigma Profile	9
2.2.2 Hydrogen Bonding	10
2.2.3 Activity Coefficient	11
2.2.4 Solubility of IL in Water	12
CHAPTER 3: METHODOLOGY / PROJECT WORK	13
3.1 Project Activities	13
3.2 Research Methodology.....	15
3.2.1 Extracting Experimental IL Inhibition Ability	15
3.2.2 Simulation of Fundamental Properties Value in COSMO-RS.....	17
3.2.3 Prediction of Inhibition Ability of Ammonium Based ILs	19
3.3 Key Milestone	21
3.4 Gantt Chart	22

CHAPTER 4: RESULTS AND DISCUSSION	23
4.1 Correlations Development and Validation	23
4.1.1 Interpretation of Sigma Profile	23
4.1.2 Hydrogen Bonding	27
4.1.3 Effect of Temperature on Predicted Inhibition Ability	39
4.1.4 Activity Coefficient	40
4.1.5 Solubility	42
4.2 Prediction of Inhibition Ability of Ammonium Based ILs ..	43
4.2.1 Sigma Profile	43
4.2.2 Total Interaction Energies	48
CHAPTER 5: CONCLUSION AND RECOMMENDATION	50
REFERENCES	52

LIST OF FIGURES

Figure 1	Schematics showing the ideal solvation process in COSMO-RS	9
Figure 2	Flowchart of steps in conducting this project	13
Figure 3	Hydrate-IL equilibrium curve from the work of Keshavarz et al	16
Figure 4	Flowchart of predicting thermodynamic properties through COSMO-RS	17
Figure 5	Inputs required to run an IL-hydrate system simulation in COSMO-RS	18
Figure 6	Flowchart showing the key milestone of Final Year Project II	21
Figure 7	Sigma profile graph of BMIM-Cl, BMIM-Br, BMIM-I and BMIM-BF ₄	24
Figure 8	Sigma profile graph of BMIM-Cl, EMIM-Cl and water	25
Figure 9	Average temperature depression from Sabil et al. work vs types of predicted energy (Binary components)	27
Figure 10	Average temperature depression against predicted hydrogen bonding energy for both EMIM and BMIM based ILs (Binary components)	28
Figure 11	Average temperature depression against predicted hydrogen bonding energy for a single data set consisting both EMIM and BMIM based ILs (Binary components)	29
Figure 12	Average emperature depression against predicted hydrogen bonding energy for ILs with Cl ⁻ as anion but different cations (Binary Components)	30
Figure 13	Average temperature depression from Sabil et al. work vs types of predicted energy (Quaternary components)	31
Figure 14	Average temperature depression from Sabil et al. work vs predicted total interaction energy (Quaternary components, without BMIM-HSO ₄)	32
Figure 15	Average temperature depression from Xiao et al. work vs predicted total interaction energy (Quaternary components)	33
Figure 16	Average temperature depression against predicted hydrogen bonding energy for ILs with Cl ⁻ as anion but different cations (Quaternary components)	33

Figure 17	Graph of predicted average temperature depression against simulation temperature	39
Figure 18	Graph of average temperature depression against $\ln(Y_w)$ for three data sets	40
Figure 19	Graph of Average Temperature Depression against Solubility of IL in Water	42
Figure 20	Sigma profile of ammonium based cations	43
Figure 21	Sigma surfaces of TMA and TBA cations	44
Figure 22	Sigma profile of anions	45
Figure 23	Sigma surfaces of OH-, Cl-, and BF ₄ -	46
Figure 24	Sigma profile of several ammonium based ILs	46

LIST OF TABLES

Table 1	Chosen papers for experimental values for this work	15
Table 2	Example of calculation of mole fraction	18
Table 3	List of ammonium based ILs being predicted	19
Table 4	Gantt Chart showing the working plan of FYP II	22
Table 5	Comparison of regression values produced by binary and quaternary components simulation	34
Table 6	Interaction energies predicted by COSMO-RS for the work of Sabil et al	35
Table 7	Experimental and predicted average temperature depression of ILs for selected literature review	36
Table 8	ILs with inconsistent experimental average temperature depression	37
Table 9.	Model summary and ANOVA for model developed	38
Table 10	Percentage difference of predicted ΔT for EMIM-Cl due to temperature difference	39
Table 11	Predicted average temperature depression of AILs	48

CHAPTER 1

INTRODUCTION

1.1 Background of Study

Gas hydrates are ice-like crystalline solid compounds that could form in the presence of water and gas under favorable thermodynamic temperature-pressure condition [1]. At condition of low temperature and high pressure, water molecules (host) will surround the gas molecules (guest) and encapsulate the gas in a hydrogen-bonded solid lattice [2]. Depending on the gases trapped, different structures of gas hydrates will be formed. Structure I hydrates trapped methane, ethane and carbon dioxide, Structure II for propane, while mixture of methane and butane will be captured by Structure H hydrates [3].

In recent decades, hydrates have received plenty of attention, because of its potential to capture and store gas. In addition, it is discovered that gas hydrates located in subsea as well as permafrost region are a potential source of energy too. However, the formation of natural gas hydrates in oil and gas pipeline is never applauded. This is because hydrates formation in pipelines have resulted in blockage and affected flow assurance of natural gas [4]. In spite of the economic losses causes by blockage, ecological disasters could occur in severe cases too. To prevent this from happening, several methods including isobaric thermal heating, water removal, depressurization, and chemical inhibitor injection [5] have been implemented. The three former methods however, are not feasible and costly. As a result, chemical inhibitors have been researched and developed a lot in recent years to control the growth of hydrates.

There are generally three types of inhibitors, which are thermodynamic hydrate inhibitor (THI), kinetic hydrate inhibitor (KHI) and anti-agglomerates (AA).

THI prevents the formation of hydrate by shifting the thermodynamic equilibrium curve of gas hydrate to a lower temperature and higher pressure [5]. KHI, on the other hand, does not inhibit hydration formation, but it slows down their nucleation and growth of hydrate. It works on the principle of lengthening the formation time of hydrate to be longer than the residence time of gas in pipelines [6]. Finally, AA, also a low-dosage inhibitor, allows the formation of hydrate, but through perturbation of water molecules, prevent the hydrates molecules to accumulate and grow larger [7].

Some common THI inhibitors include methanol and sodium chloride. In order to be effective, THI normally need to be injected in high concentration of around 10-50wt% [8], which leads to high operational cost. Furthermore, sodium chloride corrodes the oil and gas pipelines [9]. While KHI inhibitors were able to work effectively at lower dosage (<1wt%), Kelland reported that as exploration operation goes into deeper sea, KHI still has to work together with THI in order to effectively inhibit hydrate formation [7]. These limitations signify that existing chemical inhibitors are still not performing well and there is a strong need to develop more effective inhibitor [9], [10].

This leads to a recent discovery by Xiao and Adidharma in 2009, who suggested the use of IL as inhibitor due to its dual functionalities [9]. An IL inhibitor is able to shift the hydrate thermodynamic equilibrium curve to lower temperature and higher pressure, thereby making the condition for hydrate formation to be even tougher. Furthermore, it retards the formation of hydrate. Due to this great discovery, ILs have been studied a lot in the past few years. Different kinds of cation and anion pairings have been tested by means of experimental work to determine their effectiveness.

At present, experimental method is the prime method to test effectiveness of ILs as hydrate inhibitors. Besides time-consuming, an experimental work requires a high cost. Therefore, it would be good to have a predictive model based on fundamental properties that could give priori information of the effectiveness of ILs as hydrate inhibitors. It is expected that the predictive model could help in screening ILs as hydrate inhibitors or be used to validate the result of experimental work.

For this purpose, Conductor-Like Screening Model for Real Solvent (COSMO-RS), which can estimate fundamental properties of ILs system have been selected. COSMO-RS is a novel method to predict the thermodynamics properties of ILs based on quantum chemistry model [11]. Charge density of individual molecules is first calculated by COSMO-RS based on the structure of each molecule [12]. The charge density will then be distributed onto the entire molecule surface. This distribution will then be described by a one dimensional probability density [13], or more famously known as sigma profile, $P(\sigma)$. Lastly, from the charge density, chemical potential, μ will be calculated and it will act as the basis for all other calculations to predict thermodynamic properties such as Henry's law constant and activity coefficient [14]. The calculated properties will then try to be correlated to IL inhibition ability to develop a prediction model that could predict the inhibition ability of ILs.

1.2 Problem Statement

The formation of gas hydrate in oil and gas pipelines has created flow assurance problem and further resulted in the blockage of pipeline. To overcome this issue, chemical inhibitors have been widely used. Among the many types of inhibitors, ILs have been studied a lot recently as it is believed to have a good future prospect due to its dual functionalities. Nevertheless, experimental work that is the primary method in testing IL inhibition ability is costly and time consuming. Given the fact that there are limitless combinations of anions and cations to form ILs and by considering the rate of experimental work being done now, experimental testing alone is insufficient. This is because it will take an unacceptably long time until all possible ILs are tested. As consequence, the potential of IL could not be fully utilized and applied to industrial processes. Hence, a good alternative is to have predictive model that allows screening of ILs to be done based on fundamental properties. This model should be able to satisfactorily predict the inhibition ability of each IL and thus, narrow down the amount of potential ILs for experimental testing.

1.3 Objectives

Objectives refer to the goals that should be achieved by the end of project.

The main objectives of this FYP project are:

- To identify fundamental properties that affects hydrate formation
- To study the fundamental properties of IL-hydrate system through simulation using COSMO-RS
- To develop correlation between fundamental properties and inhibition ability of ILs and then validate it by comparing to experimental value extracted from peers papers
- To predict the inhibition ability of ammonium based ILs using the developed correlation

1.4 Scope of Study

In this work, hydrate system with only methane gas is investigated because it is the most common type of hydrate formed in pipelines. Followed on, the chosen fundamental properties are limited to sigma profile, hydrogen bonding, activity coefficient, and solubility of IL in water. These four properties are selected because as explained by open literature, they are understood to be able to influence gas hydrate formation. The explanation of each property could be found in the later section, literature review. Next, this work only focuses on developing correlation for thermodynamic inhibition ability of IL. When the correlation is successfully developed, the inhibition ability of 20 ammonium based ILs will be predicted.

CHAPTER 2

LITERATURE REVIEW AND THEORY

2.1 Ionic Liquids as Gas Hydrate Inhibitor

ILs are weakly coordinated compound composed by a bulky cation and an asymmetric organic or inorganic anion [12]. Due to their unique characteristic [14]–[16] such as low melting point, low flammability, negligible vapor pressure, and high thermal stability, the future applicability of ILs in many chemical process and reaction is promising. Furthermore, the presence of numerous cations and anions literally signifies limitless combinations of ions, which could then produce ILs with different properties. As a result, physical and chemical properties of ILs could be fine-tuned to meet any specific criteria and to serve any specific function [17].

In oil and gas industry, ILs was first introduced as inhibitors by Chen et al. [18] in 2008, as the team discussed about the effect of 1-butyl-3-methylimidazolium tetrafluoroborate in inhibiting CO₂ hydrate formation. A year later, Xiao and Adidharma [9] suggested the dual function of ILs inhibitors. The results showed that IL is not only able to shift the hydrate thermodynamic equilibrium curve, but it also retards the formation of hydrate. Since then, numerous experimental works have been carried out to study the effect of ILs in inhibiting gas hydrates formation, mainly using imidazolium and pyridinium based ILs [2], [3], [5], [19]. The targeted ILs of this context are ammonium based ILs (AILs), which are cheaper and easier to synthesis, but not being studied intensively. Therefore, due to cost economics and more environmental friendly, AILs are chosen to be studied in this work.

As the name implied, ammonium based ILs are made up of cation that contains the structure of NR₄⁺, where each R represents an alkyl group. Li et al. [20] conducted an experiment regarding the performance of dialkylimidazolium-based

and tetraalkylammonium-based ILs in shifting the methane hydrate thermodynamic equilibrium curve. They discovered that tetraalkylammonium-based IL with shorter alkyl substituents cation is more effective in inhibiting as compared to longer alkyl substituents cation. In addition, Li and co-worker showed that tetramethylammonium chloride performed the best as thermodynamic inhibitor, if compared to longer hydroxyethyl tetramethylammonium chloride, and three imidazolium based ILs. Furthermore, Keshavarz et al. [21] conducted a similar work, but with the use of different ILs. In the experimental results, they have showed that tetraethylammonium chloride, 1-butyl-3-methylimidazolium tetrafluoroborate and 1-butyl-3-methylimidazolium dicyanamide all displays the effect of inhibiting methane hydrate formation.

To date, all the testing work of ILs effectiveness is done using experimental method, which is by measuring the average depression temperature for thermodynamic hydrate inhibitors and by measuring induction time for kinetic hydrate inhibitors. There are generally no other methods available to validate the experimental work or to pre-screen ILs in a shorter time. Due to this reason, it is very desirable if a theoretical method to predict ILs effectiveness as hydrate inhibitors could be established just by analyzing their fundamental properties. And to obtain these fundamental properties, COSMO-RS, a thermodynamic properties predictive tool is the best option available in the market.

2.2 Conductor-Like Screening Model for Real Solvents (COSMO-RS)

COSMO-RS was introduced by Klamt et al. [22] as a new method to predict the thermodynamic properties of fluid and liquid mixture based on quantum chemistry concept of density functional theory (DFT). In COSMO-RS, charge density, σ , of surface molecules is the basis of all functions. As the first step, charge density of all interest species are calculated and stored as data. Then, chemical potential, μ of each molecule in liquid or solvent is calculated using the charge density [15]. Lastly, other thermodynamic properties such as hydrogen bonding, gas solubility and activity coefficient are derived from the chemical potential data [14]. In simple words, by only providing the structure of molecules, charge density, σ that is needed for COSMO-RS prediction could be calculated. This signifies that COSMO-RS does not require any functional group parameter or any experimental data to work. As a result, it is able to work with virtually all ILs and mixtures, even the unusual and complex combinations [23].

Throughout the years, COSMO-RS model has been successfully applied in numerous works to predict the thermodynamic properties of systems containing ILs, such as liquid-liquid equilibrium [24], [25] and activity coefficient [12], [23]. Therefore, this has prompted a lot of screening efforts of ILs through COSMO-RS for different purpose such as determining extraction solvent and improving separating process [24], [26], [27], [28]. Grabda et al. [16], for example, has used COSMO-RS to carry out screening process for ILs that is used as extraction solvent for neodymium chloride and dysprosium chloride. Kurnia [29], on the other hand, had screened imidazolium based ILs for the separation process of benzene from n-hexane through COSMO-RS.

Other than screening work, comparison and validation work has been conducted too. Calvar et al. [24], for instance, have compared COSMO-RS prediction of LLE values of ILs with their experimental data, and found out that the end result is satisfactory. In 2007, Palomar et al. [30] reinforced the applicability of COSMO-RS in predicting density and molar volume of imidazolium-based IL when their predicted values laid close to the experimental data.

Screening of ILs for gas hydrate inhibition through COSMO-RS is a relatively new and fresh concept, yet, based on the successfulness of previous works [24]-[29] in predicting thermodynamic properties, this current work is justifiable.

Moreover, to reinforce the applicability of COSMO-RS in this work, it is found out that many work involving ammonium based ILs and bionic ILs have already been conducted through COSMO-RS [16]. In 2010, Sumon and Henni [31] performed a COSMO-RS study on the properties of ILs for CO₂ capture. In this study, 12 ammonium based cations such as tetra-methylammonium, tetra-ethylammonium and tetra-butylammonium cations are used to derive ammonium based ILs to be studied. In 2014, Grabda et al. [16] studied the effectiveness of 4400 ILs for the purpose of NdCl₃ and DyCl₃ extraction. Among the many cations used are tetra-n-butylammonium, tetraethylammonium, tetramethylammonium and etc. Dodecy-dimethyl-3-sulfopropylammonium cation, which is a type of ammonium based cation, was concluded as the best performing cation in decreasing the chemical potential of NdCl₃ and DyCl₃, and thus increasing their solubility and ease the extraction process. In the same year, Pilli et al. [32] screened out the best ILs to extract phthalic acid from aqueous solution using COSMO-RS. Although ammonium based cations ILs in this simulation does not give the highest selectivity, they however, have the highest activity coefficient. Next, through COSMO-RS, Machanov á et al. [33] also obtained well-predicted values of excess molar volumes and excess enthalpy for N-alkyl-triethylammonium based ILs.

Plenty of thermodynamics properties could be studied through COSMO-RS. However, to ensure that these properties could fully and truly reflect a gas hydrate formation, several properties have been chosen carefully after conducting a thorough literature study on gas hydrates. The chosen properties are: i) sigma-profile; ii) hydrogen-bonding; iii) activity coefficient; and iv) solubility of IL in water.

2.2.1 Sigma Profile

Sigma profile, $P(\sigma)$ refers to the probability distribution of specific charge density carried by each molecular surface segment [34]. Sigma profile is crucial in this work as it allows us to understand the electronegativity and electropositivity of a molecule. It also explains about the amount of polar surface charge on a molecular surface, thereby allowing the prediction of possible interactions of the ILs in water [11].

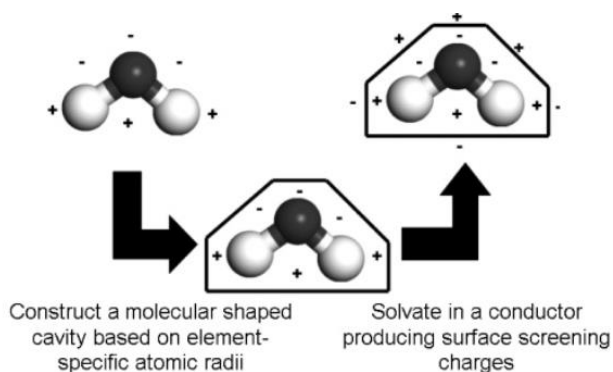


Figure 1. Schematics showing the ideal solvation process in COSMO-RS.

As shown in Figure 1, In COSMO-RS, molecule is assumed to be placed inside a cavity and then into a conducting medium. Then, the molecule's dipole will pull charges from the conducting medium to the cavity surface. These surface charges, when distributed will be known as sigma profile.

Sigma profile is also important as its graph in COSMO-RS could be used to see if an IL is hydrophobic or hydrophilic [12]. In the case of hydrate inhibitor, definitely, a hydrophilic IL is preferred, so that it would like to react with water molecules.

In the work of Palomar et al. [30], the sigma profile of ions pairs is analyzed through COSMO-RS to understand both the cation and anion effect on ILs densities. For instance, they discovered that as the number of carbon atom in alkyl group increases, the distribution of charges around non-polar area also increases. As a result, the sigma profile become less symmetric and more repulsive interactions happen between the polar and non-polar group, resulting in a harder interaction for the IL itself. In 2011, a similar work of studying ILs for CO₂ capture is done by

Sumon and Henni [31]. In their work, they analysed sigma profile of ILs to predict the available surfaces of ILs to interact with the surface pieces of CO₂.

2.2.2 Hydrogen Bonding

Hydrogen bond is formed when hydrogen interacts with two highly electronegative atoms [35]. When hydrogen bond is formed, electrostatic attraction will occur between the electronegative atom and the proton. The stronger the hydrogen bond, the harder for it to break. Thus, by having a suitable IL that creates strong hydrogen bonding with water, water will be bonded strongly and less water molecules will be free to react with gas later on [36]. Xiao and Adidharma also [9] reinforced the claim that strong electrostatic charges and hydrogen bond of ILs with water could shift the equilibrium hydrate curve and at the same time, slow down the nucleation rate of hydrate. This is supported by Xiao et al. who stated that hydrogen bonding of IL with water is strongly related to the effectiveness of IL as inhibitor [10].

In terms of COSMO-RS work, Claudio et al. [37] has obtained the calculations of hydrogen-bonding interaction energies (E_{HB}) from COSMO-RS and studied its relationship with the pairing of ions. In their work, they have proven reasonable linear relationships between hydrogen-bond basicity values and the hydrogen bonding energy. This means that the different pairing of ions could affect hydrogen bond basicity, which further has a linear correlation on hydrogen bonding energy.

Besides that, hydrogen bonding also affects other thermodynamic properties such as solubility and activity coefficient. Zhou et al. [38], for example, confirmed that hydrogen bonding interactions between anions and molecules (water) will directly affect the solubility of IL in water. In short, for the inhibition of hydrate formation, it is favorable to have an IL which ions should form strong hydrogen bonding with the water molecules. This will subsequently reduce the amount of free water molecules to form hydrate.

2.2.3 Activity Coefficient

Activity is the result of effects of ions contacting with the surrounding molecules. However, it is hard to define activity without any reference state. Therefore, ideal state is the reference state for activity. Activity coefficient is then defined as the deviation of that solution from ideal state. Generally, the higher the activity coefficient, the more responsive a molecule is. So, if water has a high activity coefficient, it means that water will interact with another molecule easily.

The formation of gas hydrate is only possible when gas and water exists at a favorable thermodynamic condition. This implies that, if water does not exist, or if water is not reacting, gas hydrate will not be formed. Thus, reducing activity coefficient of water is a way to minimize the water from reacting. By reducing the activity coefficient of water, the interaction of water molecules and methane gas will reduce, and later on formation of hydrate will be even harder.

One of the most pioneer work in predicting activity coefficient values through COSMO-RS were done by Klamt et al. [17] in 2003, which activity coefficient of organic solvents was predicted at infinite dilution in ILs using COSMO-RS. The success in obtaining close agreement between predicted values and experimental data for 38 organic solvents has since then spurred the usage of COSMO-RS. Kurnia et al in 2014 [23], again conducted a study to evaluate the accurateness of COSMO-RS in predicting water activity coefficient for ILs system. In their work, they explained that the more favorable intermolecular interactions between IL and water, the lower the water activity coefficients at infinite dilution in IL. Their statement indicates that an effective IL is supposed to interact closely with the water, and thereby lowering the activity coefficient of water. As a result, the water molecules could not have any further interaction with other molecules and thus reduce the formation of hydrate. This statement is backed by Khan et al. [12], which also stated that if activity coefficient of water in IL-water mixture is lower than 1, this implies a favorable interaction between water and the tested IL.

2.2.4 Solubility of IL in Water

Solubility of IL in water explains about how miscible IL is with the water molecules. Solubility of IL in water is an important parameter to study in gas hydrate formation as an easily miscible IL inhibitor will be able to dissociate into water rapidly, thereby starting to bond with the water [39]. The more bonding formed between IL and water, the more stable the water molecules is, thereby reducing their tendency to further interact with gas molecules to form gas hydrate. This statement is supported by Swatloski et al. [40] who in their work showed that mutual solubility of IL and water is important in affecting the rate and selectivity of reactions like formation of hydrogen bonding. They also proved that the mutual solubility of IL and water is significant in affecting the solubility of third component, which in this study, the third component will be methane or carbon dioxide gas.

In terms of applicability of COSMO-RS, Kholod et al. [41] has studied the solubility of nitro compounds in water by manipulating the temperature and salinity using COSMO-RS. Machanová et al. [42], later on, also predicted the mutual solubilities of AILs with water through COSMO-RS and compared the values with experimental data, which appeared both of the values were quite closely reflected. A similar work is later conducted by Zhou et al. [38] using COSMO-RS where the team found out that the stronger the hydrogen bond between anion and water, the higher the hydrogen bond energy, and thus a higher solubility would be achieved. They also suggested the use of short, monobranched alkyl group as cations to increase the miscibility of IL with water.

CHAPTER 3

METHODOLOGY / PROJECT WORK

3.1 Project Activities

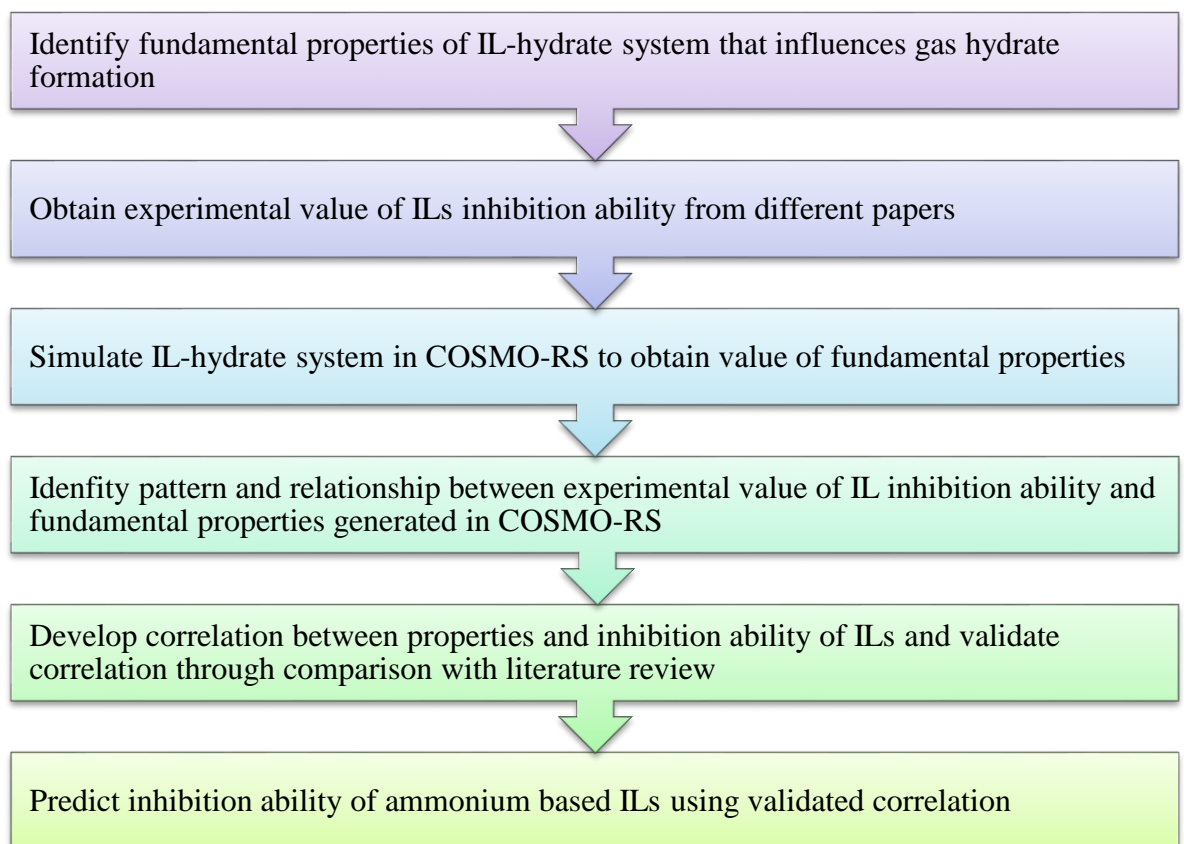


Figure 2. Flowchart of steps in conducting this project.

Basically, by the completion of this project, a correlation should be developed to depict the relationship between IL inhibition ability and the fundamental properties. Here, IL inhibition ability serves as the controlled variable, while fundamental properties are the manipulated variables. In order to develop a correlation, there should be a set of data which contains the value of these variables.

The values of controlled variable, IL inhibition ability will be obtained from several well established literature reviews. Experimental values from literature review are chosen for this project due to two reasons: i) development of correlation based on experimental values from well recognized papers serve as a validation work and this allows a better acknowledgement of the developed correlation; ii) the limited timeline of this project unable the author to carry out time consuming experiment to collect data.

On the other hand, the manipulated variables comprise four types of fundamental properties including sigma profile, hydrogen bonding, activity coefficient and solubility of IL in water. These four types of properties are selected based on literature review, and have been reported to have an effect on hydrate formation. The values of these fundamental properties could be obtained through COSMO-RS simulation. From the software, it is possible to simulate a system similar to IL-hydrate phase and then study on the fundamental properties of the system.

When the values of both variables have been collected, the next step is to plot graphs and identify the relationship between the controlled variable and the manipulated variables. Their relationship could be easily recognized if the regression value of the graph is close to 1. For instance, a graph with $R^2=0.9$ signifies that the linearity relationship is very good. Moving on, if the relationship does exist, a correlation could be developed now. In this work, correlation (equation) is developed through the help of software Minitab, which utilizes a multiple regression analysis to calculate out the constants of equation. Finally, to test the validity of this correlation, more experimental values of IL inhibition ability will be obtained from other literature reviews. These experimental values will then be compared with the predicted values that are calculated through correlation. The percentage of difference will then be computed to see if this correlation can satisfactorily predict IL inhibition ability.

3.2 Research Methodology

In the previous section, the entire process activities have been generally explained. Now, in research methodology, several activities will be described in even detailed and specific manner.

3.2.1 Extracting Experimental IL Inhibition Ability

As a relatively new study, it is very important to gain acknowledgement and recognition from peers. Hence, as mentioned earlier, the experimental value of IL inhibition ability will be obtained from several past studies that are highly recognized. For instance, paper from Xiao et al. is chosen as it is the pioneer of ILs inhibitor research. The full list of papers that were chosen for development or correlation and later for validation work is shown in Table 1 below.

Table 1. Chosen papers for experimental values for this work.

No.	Authors	Gas	Tested for
1.	Xiao et al. [10]	CH ₄	THI
2.	Sabil et al. [5]	CH ₄	THI
3.	Keshavarz et al. [21]	CH ₄	THI
4.	Zare et al. [43]	CH ₄	THI

As observed from the table, experimental values from four papers will be collected. All of them studied about hydrate formation in the presence of methane gas for the thermodynamic hydrate inhibitor. In all these papers, the effectiveness of an IL as THI was reported in the form of IL-hydrate equilibrium curve. An IL-hydrate equilibrium curve generally can be separated into a region of hydrate formation and a hydrate free region. An effective IL should then increase the pressure and lower temperature of IL-hydrate equilibrium curve, so that the region of hydrate formation becomes smaller. This action of lowering temperature can also be reported in another format, which is the average temperature depression. Generally, a larger temperature depression signifies that the IL is good in inhibiting and shifting the equilibrium curve. However, since IL-hydrate equilibrium curve is not quantifiable and thus is not possible to develop correlation, average temperature

depression will be used to represent IL inhibition ability in our work. This average temperature depression value can be calculated through the following equation [10]:

$$F = \frac{\sum \Delta T}{n} = \frac{\sum_{i=1}^n (T_{0,pi} - T_{1,pi})}{n} \quad (1)$$

where $T_{0,pi}$ is the dissociation temperature of methane in a blank sample without IL and $T_{1,pi}$ is the dissociation temperature of methane in a sample with IL inhibitor. The values of both dissociation temperatures should be obtained from the same p_i and n refers to the number of pressure point considered. For example, Figure 3 below shows the IL-hydrate equilibrium curve from Keshavarz et al. [21] for blank hydrate system (without IL) and hydrate system with BMIM-BF₄. Now, it is seen that with IL that act as inhibitor, the region of hydrate formation has reduced. It is also clear that the favorable pressure for hydrate to form has increased and the favorable temperature has reduced. This in turn made it hard for hydrate to form. Now to calculate average temperature depression, for instance at 4MPa, $T_{0,pi}$ is equal to the temperature of blank hydrate without IL, the temperature would be around 277.5K. On the other hand, $T_{1,pi}$ that refers to temperature of IL-hydrate system will be around 277K. The difference between these two values is then the temperature depression. Several temperature depression values will be collected at different pressure points along the curve. Lastly the average of these values will become the average temperature depression value.

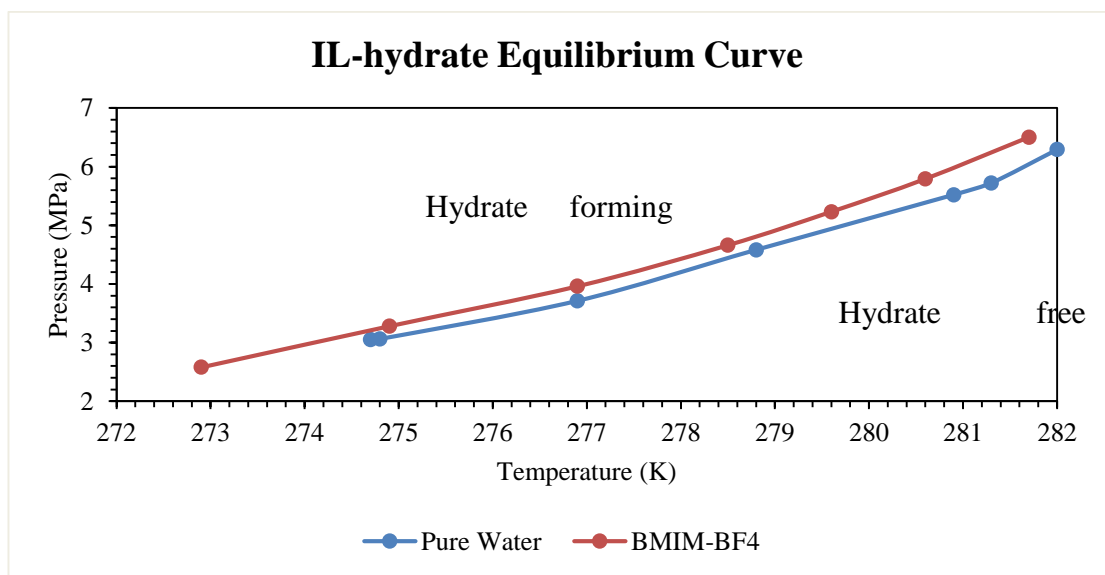


Figure 3. Hydrate-IL equilibrium curve from the work of Keshavarz et al.

3.2.2 Simulation of Fundamental Properties Value in COSMO-RS

After obtaining the data of IL inhibition ability, now it is the time to collect another set of data, which is the fundamental properties value of IL-hydrate system. Here, COSMO-RS software will be used to carry out simulation. In COSMO-RS, all calculation works are performed based on density functional theory (DFT), utilizing the triple-zeta valence polarized (TZVP) basis set [44]. Figure 4 shows the entire computational method of COSMO-RS.

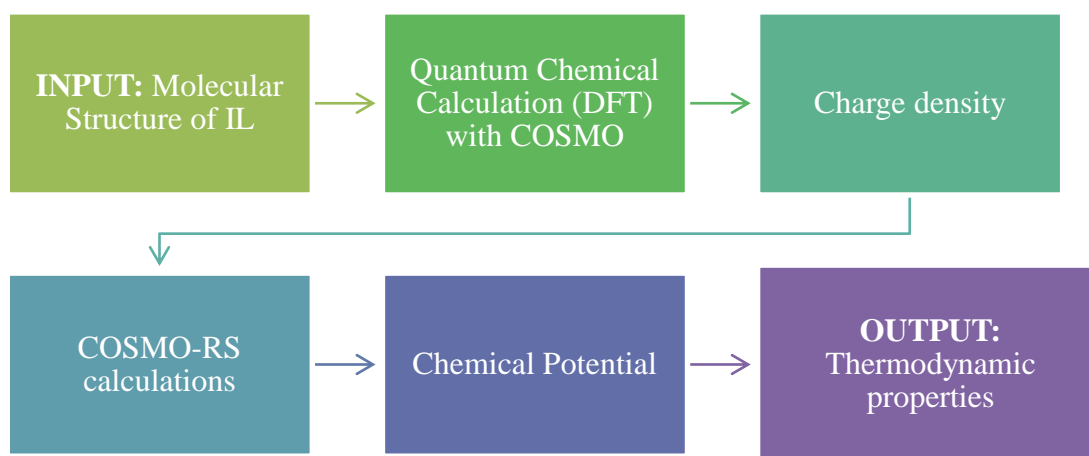


Figure 4. Flowchart of predicting thermodynamic properties through COSMO-RS.

As regard to Figure 4, COSMO-RS first requires the input of molecular(s) structure [45]. After this, the charge density of a segment on each molecule surface will be calculated in a virtual conductor. The distribution of this charge density on the entire surface of molecule will then generate sigma profile (σ -profile) through the use of COSMOtherm software [46]. Then, the σ -profile will now be used as the basis by COSMO-RS to predict the desired thermodynamic properties. Nevertheless, it is to be noted that among the computational process being shown in Figure 4, a user is only required to insert the input while all the computational process will be carried out by the software itself. Therefore, it is utmost important to input the right information in order to extract the desired output.

The input or simulation method of COSMO-RS in this work has been conducted by referring to the work of Kurnia et al [23], [47]. Figure 5 below shows

the required input for calculating hydrogen bonding value before a proper simulation could be run.

The screenshot shows the COSMO-RS software interface. On the left, there is a vertical menu with options: Mixture, Vapor Pressure, Boiling Point, Activity Coefficient, Henry Constant, Gas-Solubility, Solubility, Solvent Screening, Salt Solubility, Salt Solubility Screening, and log P / log D. The main area is divided into 'Temperature' and 'Solvent' sections. The 'Temperature' section has a text input field containing '10', a radio button selected for 'Degree C', and unselected radio buttons for 'Kelvin' and 'Fahrenheit'. The 'Solvent' section has a radio button selected for 'Mole fraction' and an unselected one for 'Mass fraction'. Below this, there is a table with four rows, each representing a component. Each row has a checkbox labeled 'Pure', a text input field for the mole fraction, and a horizontal slider. The components and their mole fractions are: 1. 1-ethyl-3-methyl-imidazolium_cation (0.0067), 2. cl_anion (0.0067), 3. h2o (0.9865), and 4. methane (0.0). Red boxes highlight the temperature input and the solvent mole fraction table.

Figure 5. Inputs required to run an IL-hydrate system simulation in COSMO-RS.

As observed from Figure 5, the required inputs are temperature, and the mole fraction of IL-hydrate system. For this work, the temperature is fixed at 10°C, which is the normal temperature where hydrate will start to form. The effect of temperature is also proven not to be significant in this work, which will be explained later in the section of result and discussion. Next, the right value of mole fraction has to be entered for all four components including cation, anion, water, and the involved gas. These mole fractions value need to be calculated beforehand as shown in the Table 2 below. Similar to experimental method that have been carried out by the chosen papers [5], [10], [21], [43], this simulation also considers that IL is inserted into water at a mass fraction 10wt%. Besides, since COSMO-RS considers IL is made up of equimolar cation and anion, a mole of IL will be divided equally into half mole of cation and half mole of anion in the calculation [14], [15], [17].

Table 2. Example of calculation of mole fraction.

Molar mass of BMIM-BF ₄	226.03g/mol
Molar mass of water	18g/mol
Assuming 100g of mixture and IL is inserted at mass fraction of 10wt%, then 90g will be water and 10g will be IL.	
Mole of water	90g / (18g/mol) = 5mol
Mole of BMIM-BF ₄	10g / (226.03g/mol) = 0.044mol
Mol fraction of water	5/(5+0.044) = 0.9912
Mol fraction of BMIM-BF ₄	0.044/(5+0.044)=0.0088
Mol fraction of anion / cation	0.0088/2=0.0044

When all inputs are inserted, the simulation can now be run. Similar simulation method will be applied for all other desired properties including sigma profile, activity coefficient and solubility of IL in water. When all fundamental properties value are collected, the next step will be identification of pattern and later, development of correlation using multiple regression analysis.

3.2.3 Prediction of Inhibition Ability of Ammonium Based ILs

In total, 20 ammonium based ILs have been selected for this study based on literature review. For cations, only shorter alkyl chains cations starting from tetramethylammonium up to tetrabutylammonium cations are chosen due to the fact that longer cations are not effective [10], [9]. This might due to the fact that shorter alkyl chains are easier to be adsorbed by crystal surface. Longer alkyl chain on the other hand, might even promote the formation of hydrates due to their increased hydrophobicity to react with water [48]. On the other hand, anions are made up of halide group, tetrafluoroborate $[\text{BF}_4]^-$ and hydroxide $[\text{OH}]^-$ ions due to their strong electrostatic charges and tendency to form hydrogen bonding with water [10].

Table 3. List of ammonium based ILs being predicted.

No	Name of IL	Molecular Formula
.		
Ammonium based ionic liquids (AILs)		
1	Tetramethylammonium hydroxide (TMA-OH)	$\text{C}_4\text{H}_{13}\text{NO}$
2	Tetraethylammonium hydroxide (TEA-OH)	$\text{C}_8\text{H}_{21}\text{NO}$
3	Tetrapropylammonium hydroxide (TPA-OH)	$\text{C}_{12}\text{H}_{29}\text{NO}$
4	Tetrabutylammonium hydroxide (TBA-OH)	$\text{C}_{16}\text{H}_{37}\text{NO}$
5	Tetramethylammonium tetrafluoroborate (TMA- BF_4)	$\text{C}_4\text{H}_{12}\text{BF}_4\text{N}$
6	Tetraethylammonium tetrafluoroborate (TEA- BF_4)	$\text{C}_8\text{H}_{20}\text{BF}_4\text{N}$
7	Tetrapropylammonium tetrafluoroborate (TPA- BF_4)	$\text{C}_{12}\text{H}_{28}\text{BF}_4\text{N}$
8	Tetrabutylammonium tetrafluoroborate (TBA- BF_4)	$\text{C}_{16}\text{H}_{36}\text{BF}_4\text{N}$

9	Tetramethylammonium chloride (TMA-Cl)	C ₄ H ₁₂ ClN
10	Tetraethylammonium chloride (TEA-Cl)	C ₈ H ₂₀ ClN
11	Tetrapropylammonium chloride (TPA-Cl)	C ₁₂ H ₂₈ ClN
12	Tetrabutylammonium chloride (TBA-Cl)	C ₁₆ H ₃₆ ClN
13	Tetramethylammonium bromide (TMA-Br)	C ₄ H ₁₂ BrN
14	Tetraethylammonium bromide (TEA-Br)	C ₈ H ₂₀ BrN
15	Tetrapropylammonium bromide (TPA-Br)	C ₁₂ H ₂₈ BrN
16	Tetrabutylammonium bromide (TBA-Br)	C ₁₆ H ₃₆ BrN
17	Tetramethylammonium iodide (TMA-I)	C ₄ H ₁₂ IN
18	Tetraethylammonium iodide (TEA-I)	C ₈ H ₂₀ IN
19	Tetrapropylammonium iodide (TPA-I)	C ₁₂ H ₂₈ IN
20	Tetrabutylammonium iodide (TBA-I)	C ₁₆ H ₃₆ IN

All the above chemicals will be simulated and calculated in COSMO-RS, which the calculations were carried out using TURBOMOLE6.1. The quantum chemical calculation follows the density functional theory (DFT), using the BP functional B88-86 with a triple-zeta valence polarized basis set (TZVP) and the resolution of identity standard (RI) approximation.

3.3 Key Milestone

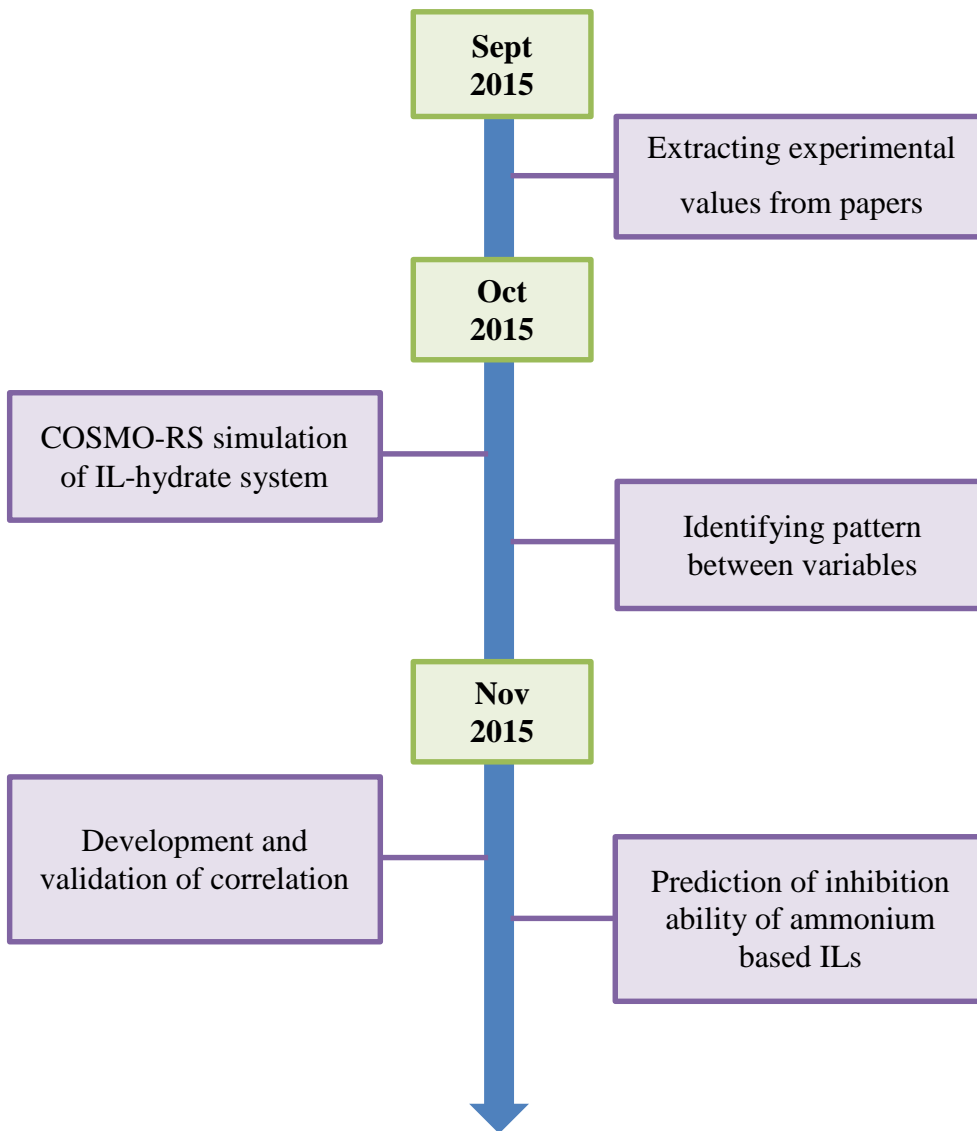


Figure 6. Flowchart showing the key milestone of Final Year Project II.

3.4 Gantt Chart

Table 4. Gantt Chart showing the working plan of FYP II.

Title	Week													
	1	2	3	4	5	6	7	8	9	10	11	12	13	14
Extracting experimental values from papers	█													
COSMO-RS simulation of IL-hydrate system		█	█											
Process and analyse simulation results regarding fundamental properties			█	█	█									
Identify pattern and relationship between fundamental properties and inhibition ability				█	█	█								
Development and validation of correlation							█							
Preparation of progress report						█	█	█						
Prediction of ammonium based ILs inhibition ability									█	█				
Pre-SEDEX										█	█			
Preparation of softbound dissertation and technical paper										█	█	█		
Preparation of FYP II Viva												█	█	
Preparation of hardbound dissertation													█	█

CHAPTER 4

RESULTS AND DISCUSSION

4.1 Correlations Development and Validation

Using the four fundamental properties that have been identified earlier, effort to relate them with the effectiveness of IL as hydrate inhibitor has been carried out. These four properties are sigma profile, hydrogen bonding energy, activity coefficient and solubility of IL in water. The following chapter will now thoroughly report and discuss if these four fundamental properties have successfully been related to IL inhibition ability.

4.1.1 Interpretation of Sigma Profile

A sigma profile graph in COSMO-RS allows us to understand certain aspects of an IL-water system. The main information we can obtain from the graph is to learn about the hydrophobicity of IL and tendency of IL to act as a hydrogen bond donor or hydrogen bond acceptor. According to Klamt [49], the sigma profile graph can be divided into three regions. First region is the hydrogen bond donor region (at the left of -1.0 e/nm^2), second region is non-polar region (between -1.0 e/nm^2 and 1.0 e/nm^2) and thirdly, hydrogen bond acceptor region (at the right of 1.0 e/nm^2). By judging at which region the peak of an IL locate, the tendency of IL to act as hydrogen bond donor or acceptor will be known. A peak that locates at the right side of sigma profile graph generally indicates more electronegative area, and act as a H-bond acceptor whereas a peak at the left side of graph indicates electropositivity.

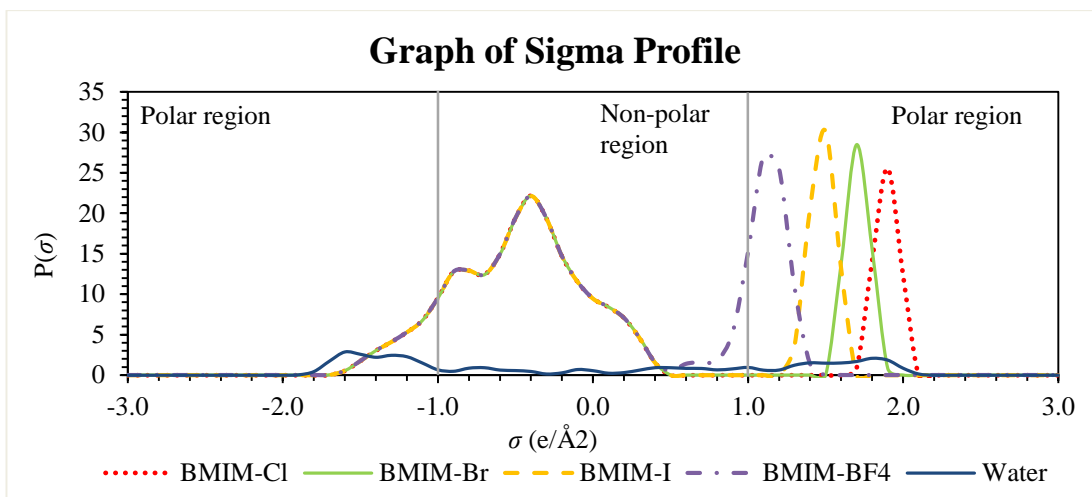


Figure 7. Sigma profile graph of BMIM-Cl, BMIM-Br, BMIM-I and BMIM-BF₄.

Now, Figure 7 shows the sigma profile graph of water molecules and four type of ILs obtained from the paper of Xiao et al. [10]. They are BMIM-Cl, BMIM-Br, BMIM-I and BMIM-BF₄. First of all, looking at the sigma profile of water molecules as shown in Figure 7, it is observed that water has two high peaks, one in the hydrogen bond donor region and another in the acceptor region [23]. This indicates that water has high affinity toward both acceptor and donor.

Moving on, looking at same cation, BMIM for these four ILs, Figure 7 shows they all can be represented by the same peak in the non-polar region. However, water molecules which have peaks in polar region, tend to have higher affinity only with strong hydrogen bond donor and acceptor, but not cation that lays its peak in the non-polar region [50]. As a result, cations actually do not interact much with water molecules. Meanwhile, anions that have their peaks in hydrogen bonding acceptor region are more attractive to water molecules. Hence, this inferred that anion is the main ion that interact with water molecules to prevent hydrate formation, whereas cation merely contribute very slightly in the process [48].

When it comes to anion, from Figure 7, it is seen all anions have their peaks at the right polar region. This indicates that they are all hydrophilic and has a high affinity to interact and bond with water molecules. Among the four anions, Cl⁻ anion has its peak furthest at the right side of graph. This highest sigma value then indicates that it is the most electronegative anion as compared to other anions. Being the most electronegative anion, this makes Cl⁻ to be more hydrophilic and is more

effective in accepting H-bond from water molecules as compared. Overall, this strongly electronegative Cl^- anion makes BMIM-Cl to be the best inhibitor among all. Looking at the position of peak in sigma profile graph, the inhibition ability is then followed by BMIM-Br, BMIM-I and finally BMIM- BF_4 . Generally, as the peak of anion become nearer and nearer to the non-polar region, the less electronegative an anion is and hence the inhibition ability reduces. This ranking deduction is supported by the experimental inhibition ability reported by Xiao et al. [10]. In their work, the experimental inhibition ability of BMIM-based ILs follows the order of BMIM-Cl > BMIM-Br > BMIM-I > BMIM- BF_4 . Hence, this actually proves the applicability of our earlier statement, which states that the further the anion peak at the right side, the higher the electronegativity of anion, and hence the better it interacts with water molecules to inhibit hydrate formation.

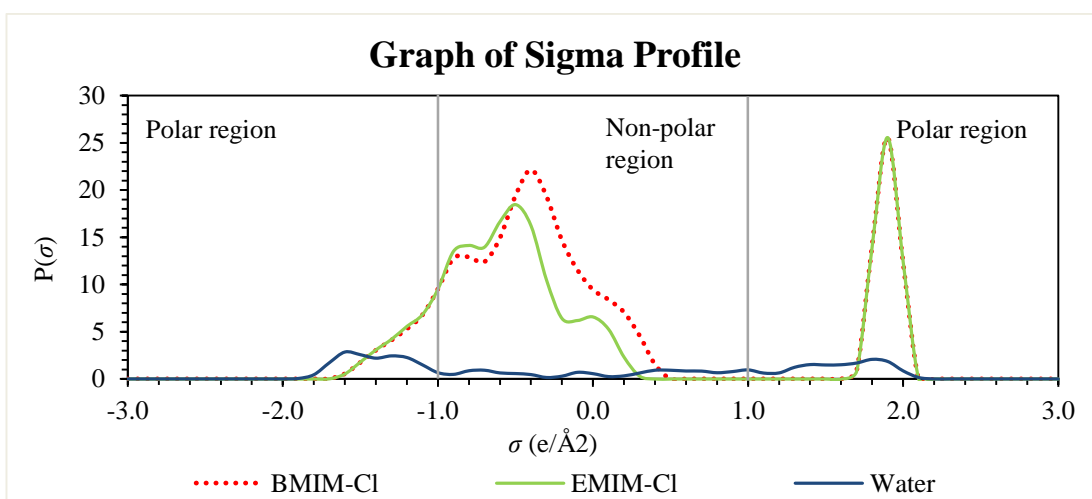


Figure 8. Sigma profile graph of BMIM-Cl, EMIM-Cl and water.

Next, Figure 8 shows the sigma profile graph of water molecules, BMIM-Cl and EMIM-Cl. This graph is plotted to see the effect of different cations on sigma profile. As observed, both ILs have the same peak for the Cl^- anion at polar region. The cations however have slightly different peaks. EMIM, which has a shorter alkyl chain length, has its peak nearer to the polar region as compared to BMIM. As consequences, EMIM is also more polarized and hydrophilic as compared, which is a desired characteristic of good hydrate inhibitor. This also proves that a cation with shorter alkyl chain length is preferable during the tuning of IL inhibitor, as a shorter cation is less bulky and hence can more effectively interact with water molecules [21], [51]. Hence, from this graph, it is clearly shown that the further the cation peak

to the left polar region, the more non-polar it is, and hence, the better it interacts with water. This will result in higher inhibition ability. Therefore, from the graph, it can be known that EMIM-Cl is a better inhibitor than BMIM-Cl. This deduction is supported by the work of Xiao et al, which reported that the inhibition ability of EMIM-Cl is better than BMIM-Cl.

In short, from sigma profile graph, the affinity of IL towards water molecules could be identified and ranked. It allows us to qualitatively study the effectiveness of IL and screen out those that are ineffective. To act as an effective inhibitor, the IL should have high affinity towards water molecules. A good anion for inhibitor should have its peak at the furthest right side because it will be very electronegative and hence can bond with water molecules well. A good cation, on the other hand, should ideally have its peak away from non-polar region, so that it is not hydrophobic to water molecules and hence hinder the interaction of IL with water.

4.1.2 Hydrogen Bonding

Although hydrogen bonding strength has been widely quoted to have relationship with the effectiveness of IL as hydrate inhibitor [9], [10], so far, no work has been conducted to prove this relationship. In this work, validation is done and has successfully proved that a linear relationship exist between hydrogen bonding strength and the effectiveness of IL as hydrate. This linearity is validated through four different sets of data that comes from three papers [5], [10], [20]. All four sets of data shows good linearity relationship, with the highest regression value as $R^2 = 1$, and the lowest as $R^2 = 0.8926$. As a result, this implies that prediction of IL effectiveness could be done through the comparison of hydrogen bonding strength.

Besides proving this relationship, several interesting findings have also been observed throughout the process. Firstly, computation of COSMO-RS, in total will calculate three kind of energy value for an IL, namely misfit energy (E_{MF}), hydrogen bonding energy (E_{HB}), and van der Waals energy (E_{vdW}). The summation of these three energies leads to the value of total interaction energy (E_{int}). Although hydrogen bonding strength is known to affect the effectiveness of IL, the significance of other energies could not be neglected yet. Hence, in Figure 9, all types of predicted energies including E_{MF} , E_{vdW} , E_{HB} and E_{INT} are plotted against average depression temperature to determine if these energies could also affect the effectiveness of ILs as hydrate inhibitor.

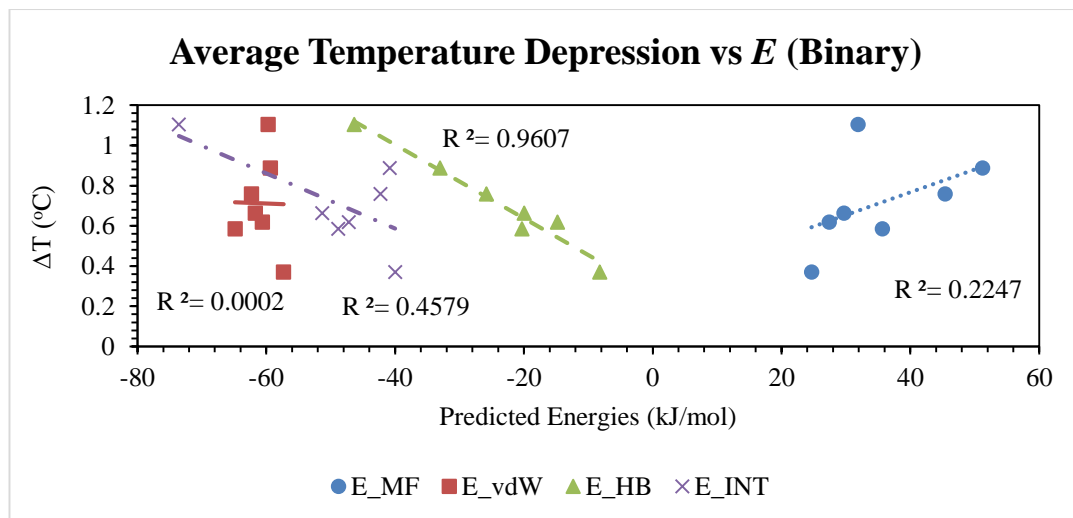


Figure 9. Average temperature depression from Sabil et al. work vs types of predicted energy (Binary components).

From Figure 9, it is evidently that van der Waals energy is nearly constant for all of the tested BMIM-based ILs and has thus no effect on the temperature depression. The contribution of misfit energy, having only a regression value of 0.2247 is also negligible. This leaves the hydrogen bonding energy to be the only energy that plays an important role in affecting the effectiveness of IL. Furthermore, the relationship between total interaction energy (E_{INT}) and temperature depression is also not convincing. This graph hence supports the earlier statement that hydrogen bonding strength between cation and anion is the most important type of energy that regulates IL interaction with water molecules [9], [10], [36]. The same pattern of relationship is then also observed in another two data sets from the work of Xiao et al. [10]. Figure 10 now shows the relationship between average temperature depression of ILs and the predicted hydrogen bonding energy from COSMO-RS.

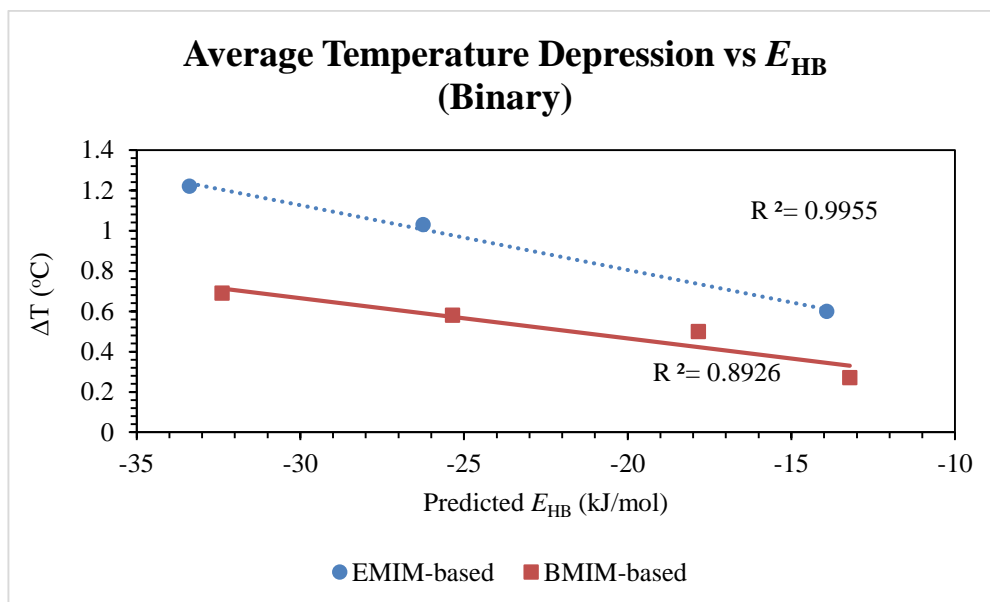


Figure 10. Average temperature depression against predicted hydrogen bonding energy for both EMIM and BMIM based ILs (Binary components).

Clearly, the graph above shows that the temperature depression value of IL-hydrate system is directly proportional to the hydrogen bonding energy (E_{HB}) for both EMIM based and BMIM based ILs. The larger the absolute value of E_{HB} , the higher the temperature depression of a hydrate system. For instance, for BMIM-based ILs in this graph, the rank of E_{HB} from highest to lowest is as BMIM-Cl > BMIM-Br > BMIM-I > BMIM-BF₄. The same ranking occurred to the average temperature depression as well, where BMIM-Cl has the highest temperature depression and BMIM-BF₄ has the lowest depression. This ranking could be

explained by the fact that among four anions, Cl^- anion has the highest polarized charge, and thus act as the best hydrogen bond acceptor. BF_4^- anion on the other hand, has the lowest polarized charge after Br^- and I^- anion, and thus shows the lowest hydrogen bond strength because it is the weakest hydrogen bond acceptor among all. This graph, however also displays an interest finding, which is the separation of EMIM and BMIM based ILs into two different data sets, instead of one. This step is necessary as the combination of all ILs into one data set may lower the linearity of relationship. This statement is supported by Figure 11, which shows a graph of average temperature depression against predicted hydrogen bonding energy.

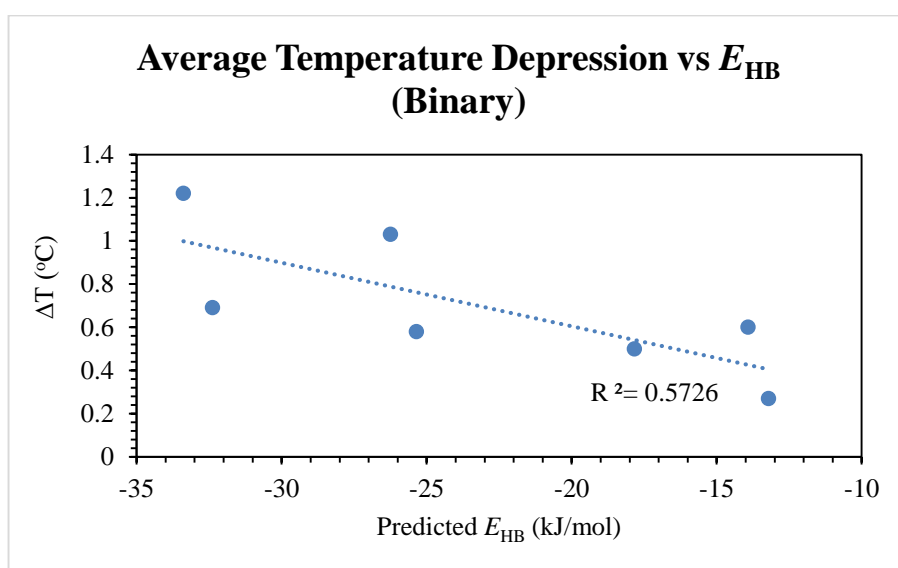


Figure 11. Average temperature depression against predicted hydrogen bonding energy for a single data set consisting both EMIM and BMIM based ILs (Binary components).

Figure 11 inferred that linear relationship only exists when ILs with same cation are compared. An early deduction is that to ensure a linear relationship for a set of data, only one single ion, which is either cation or anion, can vary while another one must be fixed. The relationship could not be applied to predict ILs with different cations and anions. This deduction is supported by Figure 12, which shows the regression value between average depression temperature and hydrogen bonding strength for a set of ILs with different cations but same Cl^- anion.

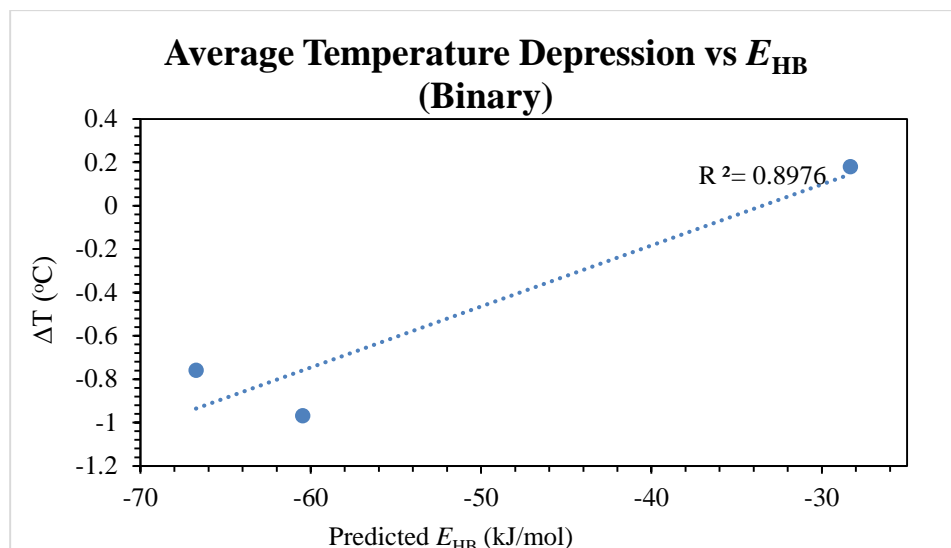


Figure 12. Average emperature depression against predicted hydrogen bonding energy for ILs with Cl⁻ as anion but different cations (Binary components).

With the regression value as high as 0.8976 from Figure 12, this supports our deduction earlier, where one ion must be fixed and another one could be varied to see the relationship. Furthermore, it is noticeable that when ILs with fixed anion but different cations are measured, the relationship between hydrogen bonding strength and average depression temperature is inversely proportional as before. The higher the absolute value of hydrogen bonding energy, the lower the average temperature depression. This could be explained by the sigma potential graph that has been discussed earlier. Previously, it is explained that cations generally have their peaks located in the non-polar region of sigma profile, which is from -1 to 1 e/nm². On the other hand, water molecules show two high peaks, one at the region of hydrogen bond donor and another at hydrogen bond acceptor. As a result, water molecules tend to have higher affinity only with strong hydrogen bond donor or acceptor, but not cation that lays its peak in the non-polar region. Hence, this inferred that anion is the main ion that interact with water molecules to prevent hydrate formation, whereas cation merely contribute very slightly in the process [48]. Since cations have low affinity with water molecules, this also indicates that most of the cations in water will continue to bond with anions. In that case, the excess hydrogen bonding energy provided by stronger cation (that has higher E_{HB}) is actually unnecessary. In fact, this stronger hydrogen bonding energy will be used by cation to bond with anion, thus reduces the amount of anions that are free to interact with water molecules. As consequence, it will bring about inverse effect on average temperature depression and reduce the effectiveness of ILs as hydrate inhibitor.

In short, linear relationship do exists between hydrogen bonding strength and the thermodynamic hydrate inhibition ability of an IL. For a set of ILs with fixed cation and different anions, stronger hydrogen bonding between ILs lead to higher average depression temperature of an IL-hydrate system. Vice versa, for a set of ILs with fixed anion but different cations, stronger E_{HB} produce lower depression temperature. A lower depression of temperature subsequently signifies that the IL is less capable to shift the equilibrium curve and is thus a weaker THI inhibitor. Predicted hydrogen bonding energy computed by COSMO-RS through a binary system consisting of only cation and anion has thus proven to be useful in predicting the effectiveness of ILs as inhibitors.

However, the above method of computation in COSMO-RS involves only the interaction between cation and anion and it does not represent the hydrate system fully. Thus, a second computation of quaternary system containing cation, anion, water and methane gas has been conducted. Similar graphs have been plotted to find out how consistent E_{HB} is in predicting the effectiveness of IL. Figure 13 below shows the graph of average depression temperature plotted against different type of predicted energies.

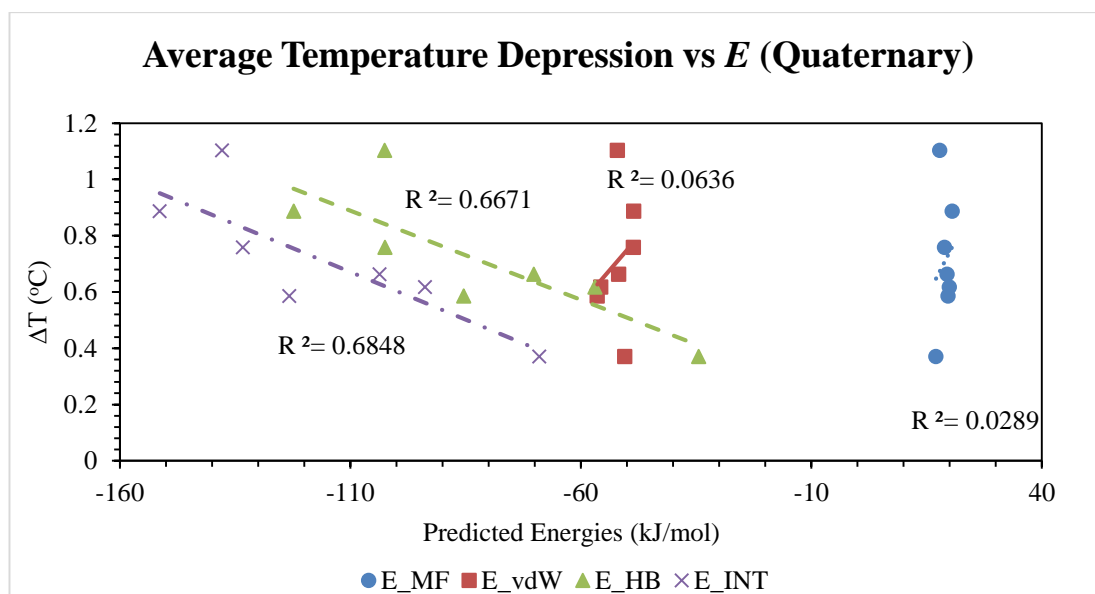


Figure 13. Average temperature depression from Sabil et al. work vs types of predicted energy (Quaternary components).

As observed from Figure 13, when quaternary components are involved, which includes cations, anions, water and methane, it is still obvious that hydrogen bonding energy (E_{HB}) is the main energy that influences the hydrate inhibition effect. Meanwhile, misfit energy and van der Waals energy have only a low regression value that is below 0.10. However, it is noticed that total interaction energy (E_{INT}) provides a slightly higher regression value than E_{HB} which is 0.6848 as compared to 0.6671, which does not occur in binary components simulation. This could be due to the fact that while involving more components such as methane and water, the van der Waals energy and misfit energy between different components are now more significant and influential. Yet, as compared to binary components regression value, the highest regression value that is obtained here is only 0.6848, which is extracted from the E_{INT} . Nevertheless, this low regression value could be improved to 0.8276 by removing the outlier which is BMIM- HSO_4 (1-butyl-3-methylimidazolium hydrogen sulfate) as shown in Figure 14. This is because of the nature of HSO_4^- anion, which has an extra hydrogen bonding functional group, OH^- (hydroxide) and thus resulting in stronger inhibition effect [36], [36].

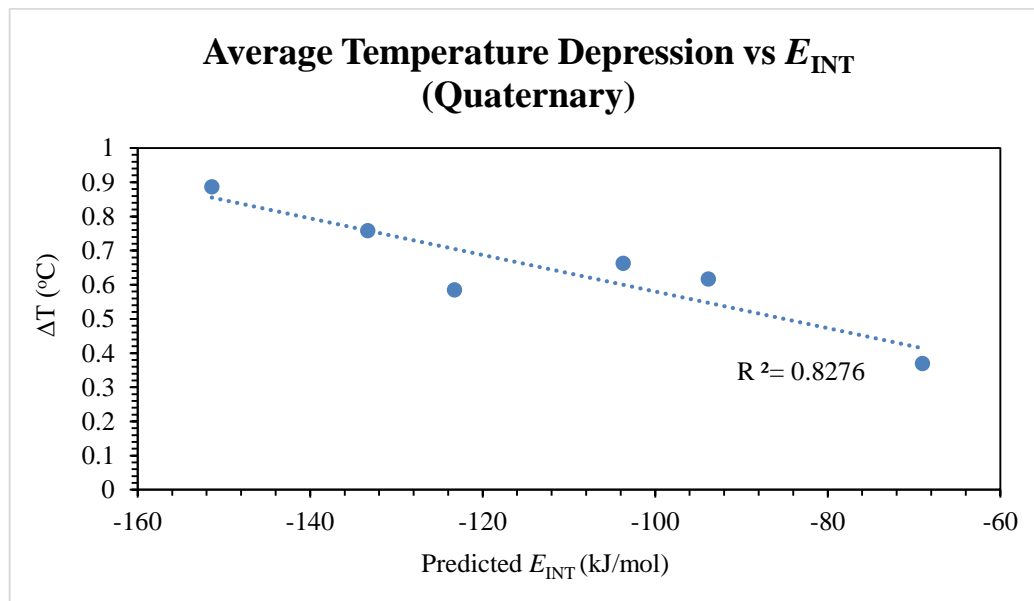


Figure 14. Average temperature depression from Sabil et al. work vs predicted total interaction energy (Quaternary components, without BMIM- HSO_4).

Figure 15 then shows the regression value of two more data sets from the work of Xiao et al [10]. For both sets of data, total interaction energy (E_{INT}) gives the highest regression value too.

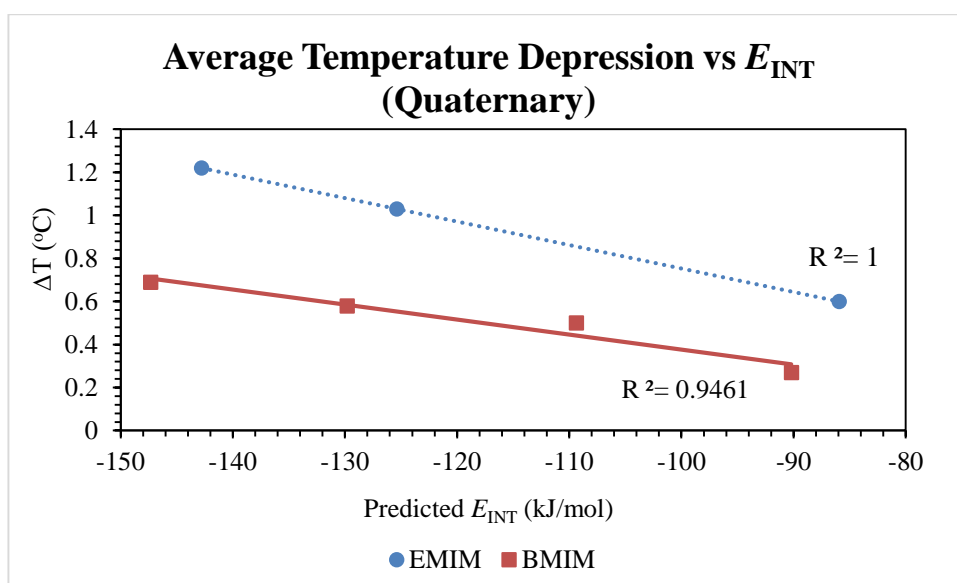


Figure 15. Average temperature depression from Xiao et al. work vs predicted total interaction energy (Quaternary components).

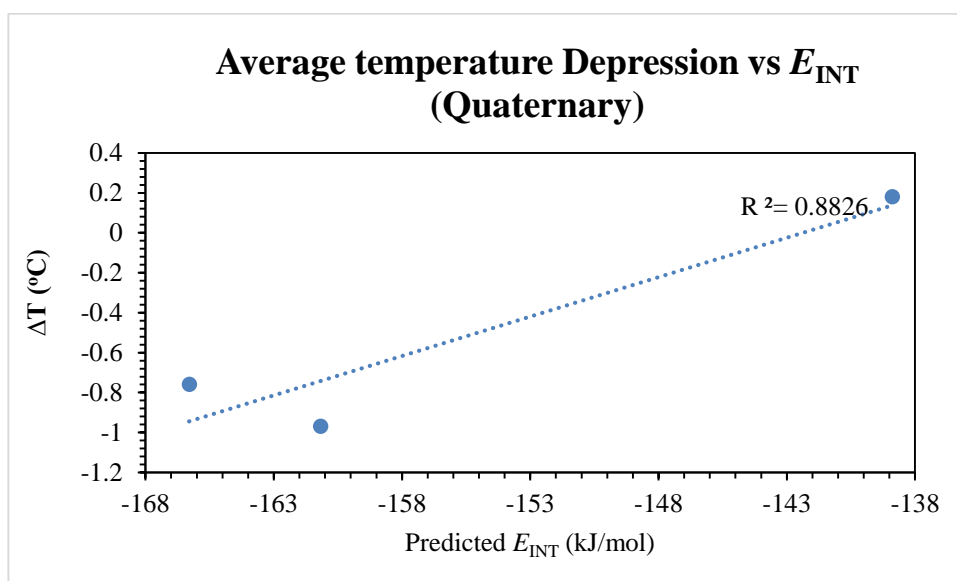


Figure 16. Average temperature depression against predicted hydrogen bonding energy for ILs with Cl⁻ as anion but different cations (Quaternary components).

Similarly, from Figure 16, when the anions are fixed, and cations are varied to study, the temperature depression value also decreases as the hydrogen bonding energy becomes more negative (stronger). Therefore, generally, COSMO-RS simulation of binary components and quaternary components both work well as a quick prediction for the effectiveness of IL as thermodynamic hydrate inhibitor.

Table 5. Comparison of regression values produced by binary and quaternary components simulation.

Sets of IL data	R ² (Binary)	R ² (Quaternary)
BMIM based ILs (Sabil et al. [5])	0.9607	0.8276
BMIM based ILs (Xiao et al.[10])	0.8926	0.9461
EMIM based ILs (Xiao et al. [10])	0.9955	1
Chloride based ILs (Li et al. [20])	0.8976	0.8826

Table 5 above shows the regression value of both binary and quaternary components simulation. Here, it is shown that simulation of hydrogen bonding energy (E_{HB}) of binary components simulation provides a more consistent regression value. On the other hand, total interaction energy (E_{INT}) of quaternary components simulation, more accurately reflect out the hydrate state which involves not only the IL itself, but also water molecules and methane gas. In order to determine whether binary or quaternary components simulation is more effective in predicting ILs effectiveness, more sets of experimental data should be validated using the above approach. However, experimental work that tested ILs set with fixed anion or cation is very limited. Therefore, it is hard to conclude here whether binary or quaternary components simulation is more superior. Nevertheless, since real hydrate system consists of the interaction between water, methane and IL, quaternary components simulation will be further studied and correlation will be developed in this work.

From the previous analysis for quaternary simulation, it is observed that total interaction energy of anion and cation has different effect on average temperature depression. Anion with higher interaction energy shows a higher average temperature depression, while the stronger interaction energy of cation reduces the average temperature depression. Due to the opposite effect of these two types of interaction energies (cation and anion), it is thus a must to consider them separately during the development of correlation. This results in the splitting of total interaction energy (E_{INT}) into two variables, which are E_{INT} contributed by anion ($E_{INT,A}$) and E_{INT} contributed by cation ($E_{INT,C}$). Both of them are available and obtainable from COSMO-RS simulation. Table 6 below shows an example of $E_{INT,C}$, $E_{INT,A}$ and E_{INT} calculated by COSMO-RS for the ILs from the work of Sabil et al [5].

Table 6. Interaction energies predicted by COSMO-RS for the work of Sabil et al.

ILs	$E_{INT,C}$	$E_{INT,A}$	E_{INT}
BMIM-Cl	-25.61552	-125.76895	-151.384
BMIM-Br	-25.86398	-107.45348	-133.317
BMIM-DCA	-26.37615	-77.31303	-103.689
BMIM-CF3SO3	-26.24535	-67.59179	-93.8371
BMIM-CH3SO4	-26.26126	-96.99914	-123.26
BMIM-CIO4	-26.20864	-42.78859	-68.9972
BMIM-HSO4	-26.19087	-111.6787	-137.87

From the table, it is clear that the summation of $E_{INT,A}$ and $E_{INT,C}$ would result in the value of E_{INT} . In comparison, it is also evidently shown that anion contributes more to the total interaction energy than the cation. Now after obtaining the two variables, Minitab is used to assist in developing a suitable correlation for the prediction of average temperature reduced by each IL. Generally, the model could be described as:

$$Y = \beta_1 + \beta_2 X_2 + \beta_3 X_3 + \dots$$

$$\Delta T = \beta_1 + \beta_2 E_{INT,C} + \beta_3 E_{INT,A}$$

Among many equations that have been tested, the best equation is listed below. It involves both $E_{INT,A}$ and $E_{INT,C}$ as independent variables.

Model:

$$\Delta T = 1.758 + 0.0643 E_{INT,C} - 0.00559 E_{INT,A} \quad (2)$$

Table 7 below then shows the experimental value obtained from literature review, as well as the predicted temperature using the above equation. It listed 25 ILs with their experimental average temperature depression value from 4 literature review [5], [10], [21], [43]. Using the values of ions' interaction energy ($E_{INT,A}$ and $E_{INT,C}$) obtained from COSMO-RS, average temperature depression has been predicted for each IL. Absolute error between experimental and predicted value is then calculated and shown at the last row of the table, without considering the three extreme outliers that are highlighted in red.

Table 7. Experimental and predicted average temperature depression of ILs for selected literature review.

Paper	ILs	Experimental ΔT ($^{\circ}\text{C}$)	Predicted ΔT ($^{\circ}\text{C}$)	Absolute Error (%)
Xiao et al. [10]	EMIM-Cl	1.220	1.125	7.75
	EMIM-Br	1.030	1.001	2.77
	EMIM-BF ₄	0.600	0.742	23.68
	BMIM-Cl	0.690	0.843	22.24
	BMIM-Br	0.580	0.727	25.32
	BMIM-I	0.500	0.593	18.64
	BMIM-BF ₄	0.270	0.473	75.35
	PMIM-I	0.800	0.731	8.66
Sabil et al. [5]	BMIM-Cl	0.887	0.843	4.91
	BMIM-Br	0.758	0.727	4.11
	BMIM-DCA	0.663	0.527	20.49
	BMIM-CF ₃ SO ₃	0.617	0.482	21.93
	BMIM-MeSO ₄	0.585	0.644	10.03
	BMIM-ClO ₄	0.370	0.348	5.88
	BMIM-HSO ₄	1.103	0.729	33.88
	[OH-C ₂ MIM]-Cl	1.329	-0.260	119.58
	[OH-C ₂ MIM]-Br	0.960	-0.373	138.88
Keshavarz et al. [21]	BMIM-BF ₄	0.858	0.473	44.79
	BMIM-DCA	0.720	0.527	26.82
	N ₂ ,2,2,2-Cl	1.080	1.218	12.80
Zare et al. [43]	BMIM-BF ₄	0.460	0.473	2.92
	EMIM-EtSO ₄	0.670	0.938	40.07
	EMIM-HSO ₄	0.990	0.999	0.95
	BMIM-MeSO ₄	1.020	0.644	36.90
	OH-EMIM-BF ₄	1.100	-0.625	156.78
Average:				20.49

Moving on, the table shows several interesting finding and limitation of the model. First, regarding the three extreme outliers, all three of them are substituted cations that have a hydroxyl (OH^-) group. This type of substituted cation, as calculated by COSMO-RS, has an overly high $E_{\text{INT,C}}$ (42.17kJ/mol for [OH-C₂MIM]-Cl as compared to 20.60kJ/mol for EMIM-Cl), which supposed to reduce their inhibition ability. But, in truth, hydroxyl group substituted cation has constantly performed better than common cation because the OH^- serves as a strong hydrogen bond donor that will react with water [20], [52]. The increased interaction with water molecules will thus improve the average temperature depression [53]. Due to this reason, a large discrepancy is observed between experimental and predicted

temperature depression for OH⁻ substituted cations based ILs. This also signifies that the model developed earlier is not applicable to hydroxyl group substituted cations or possibly any other substituted cations ILs.

Next, pure error which caused by inconsistency between experiments has also limited the accuracy of this model. Table 8 below shows the simplified list of ILs which have different experimental average temperature depression value obtained from literature review.

Table 8. ILs with inconsistent experimental average temperature depression.

ILs	Literature Review	Experimental ΔT (°C)	Predicted ΔT (°C)	Absolute Error (%)
BMIM-Cl	Xiao et al. [10]	0.690	0.843	22.24
	Sabil et al. [5]	0.887		4.91
BMIM-Br	Xiao et al.[10]	0.580	0.727	25.32
	Sabil et al. [5]	0.758		4.11
BMIM-BF ₄	Xiao et al.[10]	0.270	0.473	75.35
	Keshavarz et al. [21]	0.858		44.79
	Zare et al. [43]	0.460		2.92
BMIM-MeSO ₄	Sabil et al. [5]	0.585	0.644	10.03
	Zare et al. [43]	1.020		36.90
BMIM-HSO ₄	Sabil et al. [5]	1.103	0.729	33.88
EMIM-HSO ₄	Zare et al. [43]	0.990	0.999	0.95

As observed from Table 8, the experimental value obtained from literature review does not agree with each other. They are inconsistent and this has thus hindered the development of a fully accurate model that could predict the inhibition ability of ILs as THI inhibitors. For instance, the inhibition ability of BMIM-BF₄ was reported in three different papers and the difference of experimental value from each paper is fairly large, ranging from 0.270°C to 0.858°C. Nevertheless, Zare et al. [43] reported an experimental value of 0.460°C, which only presents a 2.92% error when compared to the predicted value.

Next, looking at BMIM-HSO₄ and EMIM-HSO₄, it is experimentally proven that EMIM-HSO₄, which has a smaller alkyl chain length for cation, would serve as a better inhibitor [21], [36], [51]. However, due to the fact that experimental values are obtained from two different papers [5], [43], BMIM-HSO₄ recorded a higher average temperature depression. This contradiction due to inconsistency again, hardened the process of model development. This inconsistency between experimental values could probably be explained by two factors: i) purity of ILs being used in experiment; ii) experimental procedure and atmospheric condition.

In short, hydrogen bonding energy is the main type of energy that affects the interaction of ions with water and subsequently the inhibition ability of ILs. For a quaternary components simulation however, total interaction energy shows a better linear relationship with average temperature depression. Model developed which considers, cation interaction energy and anion interaction energy sufficiently predicts average temperature depression with an average error of 20.49%. It is to be noted that to a certain degree, the inconsistency between experimental values also contributed to the average error. Table 9 below shows the regression statistics and P-value from ANOVA test for the equation developed. Confidence level for the model is set at 95%, and thus a P-value of 0.000 (<0.05) signifies a reliable model.

Table 9. Model summary and ANOVA for model developed.

Model Summary					
R ²	:	78.23%			
R ² (Adjusted)	:	73.88%			
Standard Error	:	0.131049			

ANOVA					
Source	DF	Adjusted SS	Adjusted MS	F-value	P-value
Regression	2	0.6173	0.30865	17.97	0.000
Residual	10	0.1717	0.01717		
Total	12	0.7890			

4.1.3 Effect of Temperature on Predicted Inhibition Ability

From earlier section 3.2.2, it is mentioned that in this work, the simulation work is fixed at a temperature of 10°C, which is a common temperature where hydrates start to form. In this section, the effect of temperature is further examined to investigate if the predicted inhibition ability of ILs changes dramatically with temperature. Figure 17 below shows the graph of predicted average temperature depression against simulation temperature.

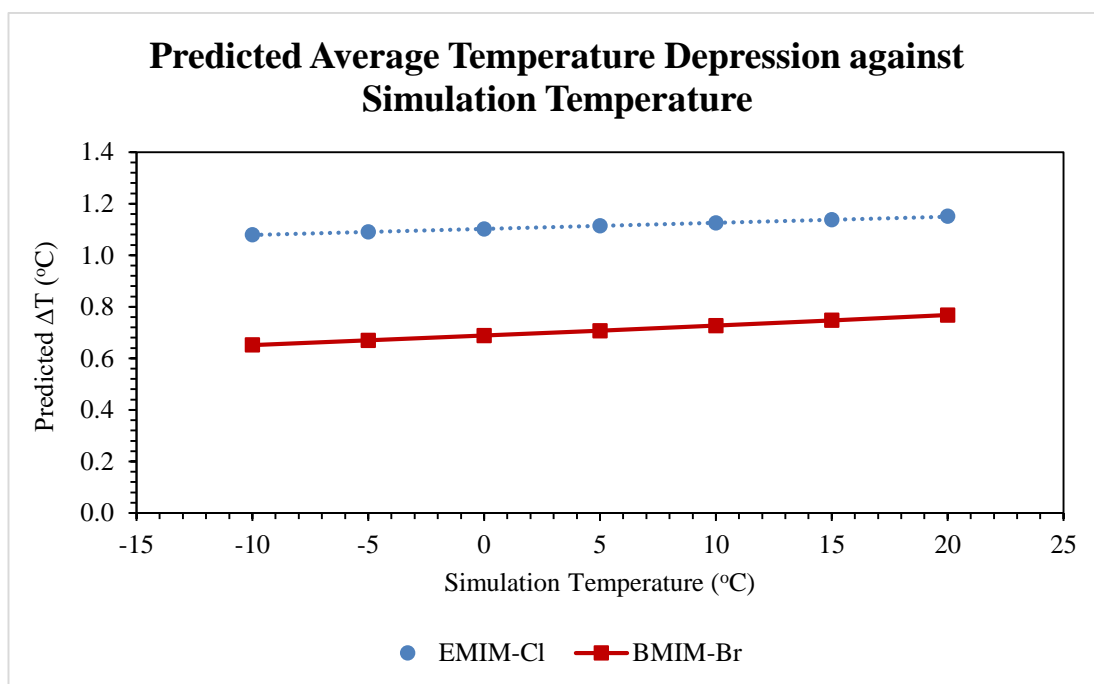


Figure 17. Graph of predicted average temperature depression against simulation temperature.

Nevertheless, if the percentage of difference is calculated out, it will be noticed that the effect of temperature is very insignificant. For example, for EMIM-Cl, using simulation of 10°C as reference state, the percentage difference for each temperature is shown at table below.

Table 10. Percentage difference of predicted ΔT for EMIM-Cl due to temperature difference.

Temperature (°C)	-10	-5	0	5	10	15	20
Predicted ΔT (°C)	1.079	1.09	1.102	1.113	1.125	1.138	1.151
Percentage difference (%)	4.10	3.12	2.11	1.07	0.00	1.10	2.24

As shown in table above, the range of predicted average temperature depression is between 1.079 to 1.151°C, where the difference is really small. Furthermore, it is found out that most experimental study involves only temperature range of -3.15°C to 16.85°C (270K-290K) [3], [9], [10], [21], [52]. This means that the highest percentage difference is just around 3.12% (for -5°C). Hence, it can be concluded that effect of temperature is insignificant and would not affect the screening process of ILs using the correlation.

4.1.4 Activity Coefficient

As discussed by Kurnia et al. [23], the lower the activity coefficient of a water-IL mixture, the higher the interaction between components in the mixture. Khan et al. also explains that for a water-IL mixture, activity coefficient below 1 signifies favourable interaction between water and ILs in the mixture [12]. When ILs interact well with water, supposedly, less water will be free to bond with each other to form hydrate. Theoretically, activity coefficient could then reflect out the inhibition ability of IL. Therefore, validation effort was done through four sets of data [5], [10], [20] to find out if the relationship between activity coefficient and average temperature depression exists. Figure 18 below shows the graph of average temperature depression against natural logarithm of activity coefficient.

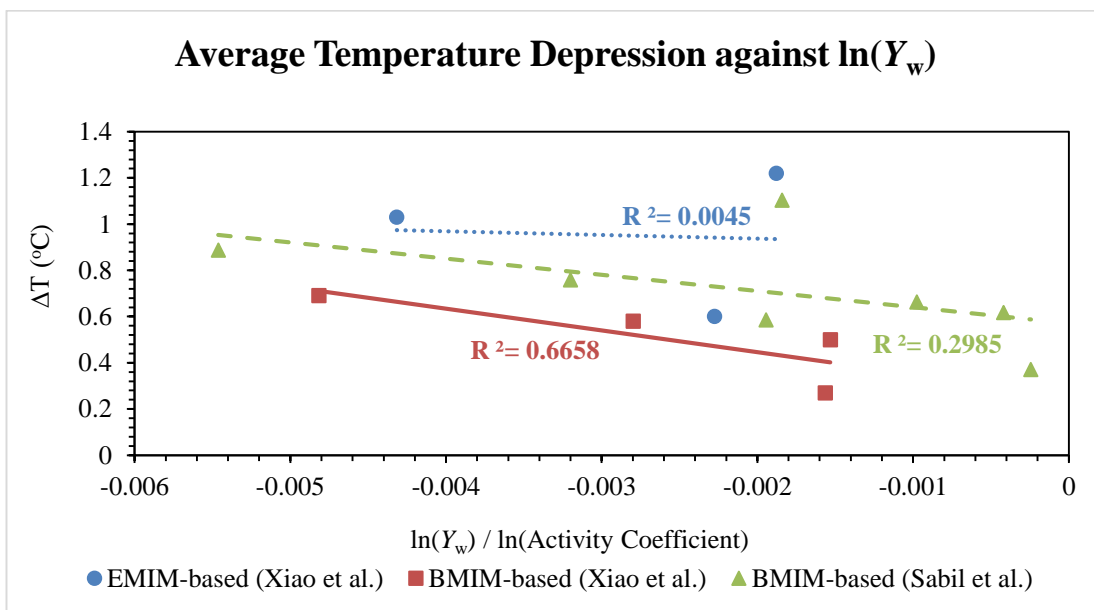


Figure 18. Graph of average temperature depression against $\ln(Y_w)$ for three data sets.

As shown in Figure 18, the highest regression value is observed for BMIM-based ILs from the work of Xiao et al, which is a mere 0.6658. Meanwhile, another two sets of data record unacceptably low regression value of only 0.0045 and 0.2989. Hence, regrettably, these three sets of data could not exhibit any significant relationship between these two variables. Nevertheless, a general pattern of decreasing average temperature depression is observed when the natural logarithm of activity coefficient increase (activity coefficient increases). The incapability of activity coefficient in reflecting the inhibition ability of IL could probably due to the fact that calculation of activity coefficient in COSMO-RS considers only the input of temperature, but no input of pressure is allowed. Meanwhile, in reality, hydrate occurs at low temperature (around 10°C) but high pressure. This kind of special nature of hydrate formation has thus made it hard for COSMO-RS to accurately predict out the activity coefficient water for a system of low temperature yet high pressure.

4.1.5 Solubility

A more soluble IL in water signifies that the IL can easily dissolve itself and interact with water molecules. Supposedly, a good IL should have high solubility in water, in order to bond with other water molecules and reduce the possibility of free water molecules from forming hydrate. In order to test the validity of the statement, four sets of data [5], [10], [20] was studied to find out if the relationship between solubility of IL in water and average temperature depression exists. Figure 19 below shows the graph of average temperature depression against solubility of IL in water.

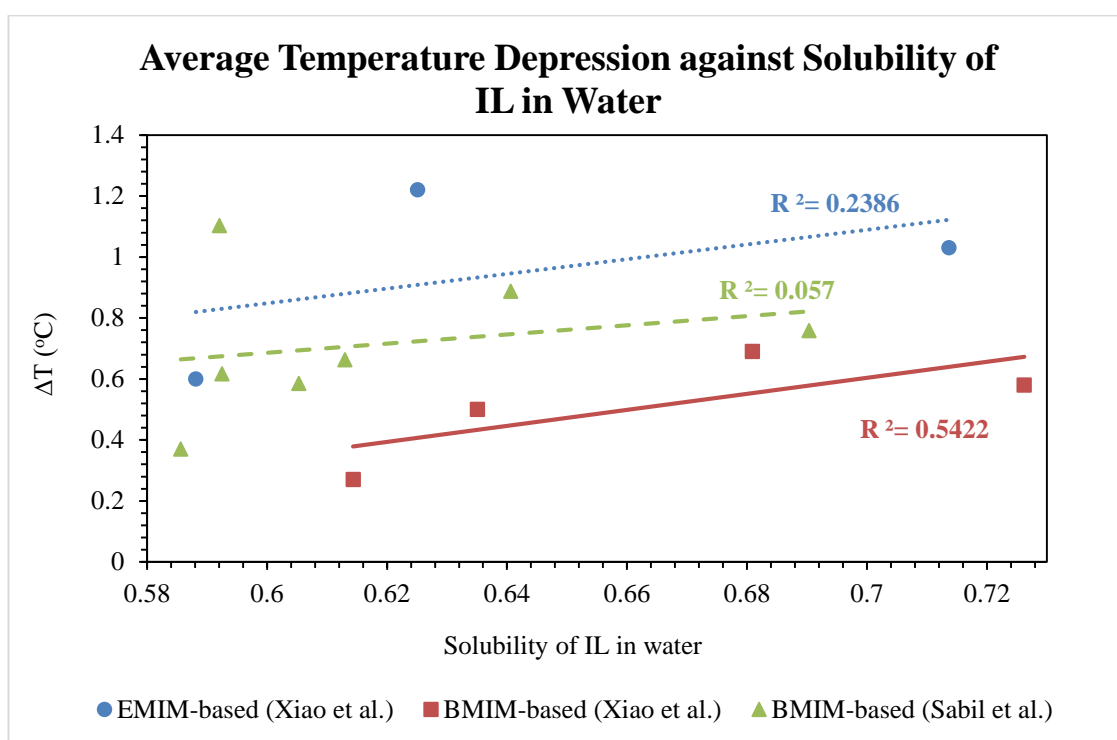


Figure 19. Graph of Average Temperature Depression against Solubility of IL in Water.

Here, the regression values for all three data sets are very low as well, with the lowest regression value of 0.057. Hence, similarly to activity coefficient, no significant relationship could be deduced from this variable.

4.2 Prediction of Inhibition Ability of Ammonium Based ILs

From the validation part, it has been confirmed that sigma profile and total interaction energy of ILs can be correlated to the effectiveness of an IL as THI inhibitor. Hence, in this section, prediction work will be conducted on 20 ammonium based ILs (refer to Table 3) to determine their ability as hydrate inhibitor, through the study of their sigma profile and total interaction energies.

4.2.1 Sigma Profile

Although sigma profile could not directly compute a value to represent the effectiveness of an IL as hydrate inhibitor, it does show the affinity of an IL towards water. The higher the affinity of IL towards water, the more hydrophilic it is, and the easier it could interact with water. This will then result in a more effective hydrate inhibitor. Hence, in this section, three sigma profile graphs will be used to determine the affinity of each ammonium based ILs towards water. The first figure, Figure 20, displays the sigma profile of the four types of cations involved here, which range from tetramethylammonium (TMA) to tetrabutylammonium (TBA).

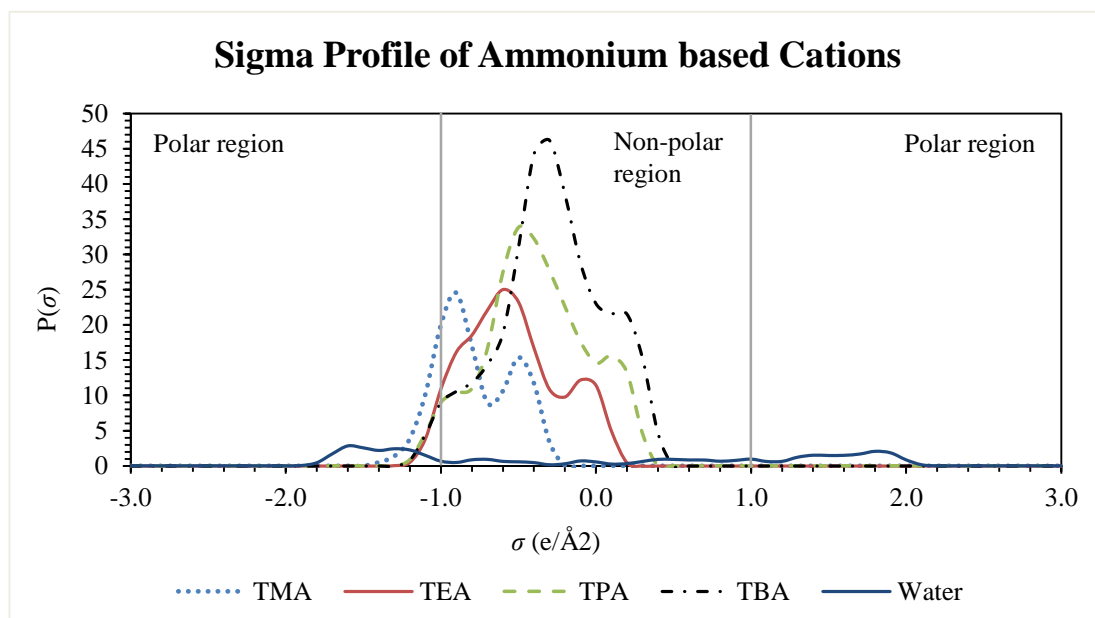


Figure 20. Sigma profile of ammonium based cations.

From section 4.1.1 Interpretation of Sigma Profile, it is discussed that the sigma profile graphs could be divided into three regions: hydrogen bond donor region (at the left of $-1.0e/nm^2$), non-polar region (between $-1.0e/nm^2$ and $1.0e/nm^2$) and hydrogen bond acceptor region (at the right of $1.0e/nm^2$). Here, all tetraalkylammonium based cations have their peaks within the non-polar region and is thus deduced to have low affinity with water. This is because water molecules have only peaks within the hydrogen bond donor and hydrogen acceptor region. Due to this property, they do not interact well with ions that have peak in the non-polar region. However, when compared among themselves, TMA cation which has its highest peak at around $-0.9e/nm^2$ performs the best because its peak is nearest to the polar region and thus has the highest affinity towards water when compared. This is because TMA has the lowest alkyl chain length, thus is less bulky and can easily interact with water molecules [12]. This makes TMA to be the most suitable cation among four to be tuned as hydrate inhibitor. This statement is supported by Figure 21, which shows the sigma surfaces of two cations, TMA and TBA. In sigma surface, the color changes from dark blue (highly electropositive) to blue (electropositive) and finally green (non-polar) [14]. Hence, to act as a good cation for inhibitor, the cation should have as less green color as possible. This is satisfied by TMA, which its major surface is in blue color (electropositive). TBA cation, on the other hand, is mostly green in color. This indicates a very non-polar cation. This phenomenon also explains why TMA is more polarized than the other three cations, and why it is the most suitable type of cation to be used.

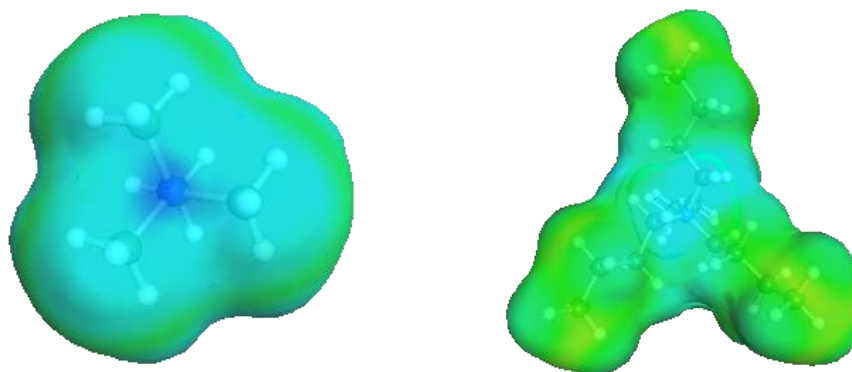


Figure 21. Sigma surfaces of TMA and TBA cations.

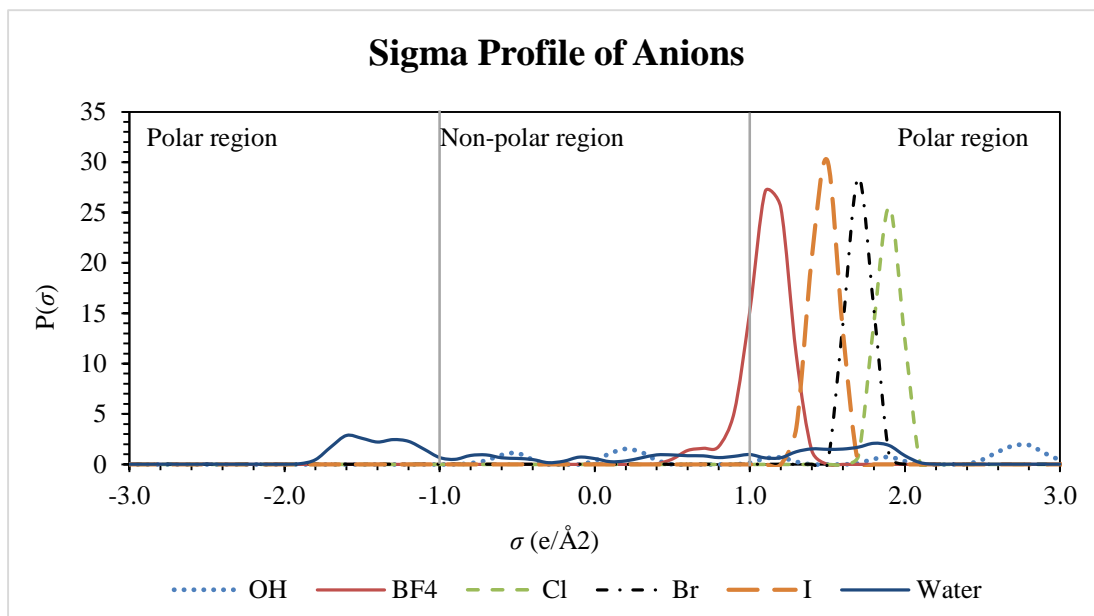


Figure 22. Sigma profile of anions.

The second figure, Figure 22 shows the sigma profile of five types of different anions. From this graph, it is observed that all anions have their peaks located in polar region at the right side, which is the hydrogen bond acceptor region [11]. This indicates that all of them are electronegative, and has a lone pair ready to share with another hydrogen bond donor. Due to their readiness to interact with hydrogen bond donor, they have high affinity with water molecules, and tend to bond well with water molecules. The highest tendency of interaction goes to OH^- ion, which has its peak at $3.6\text{e}/\text{nm}^2$. In general, anion that lays its peak further at the right side of sigma profile graph is effective in inhibiting as it has high affinity with water molecules. This is due to the fact that the further the peak to the right, the larger the sigma value and thus, the more electronegative an anion is. This statement is supported by Figure 23, which displays the sigma surface of three anions, OH^- , Cl^- , and BF_4^- . In sigma surface, brown color represents the highest electronegativity, followed by red color and finally to green color that indicates non-polar.

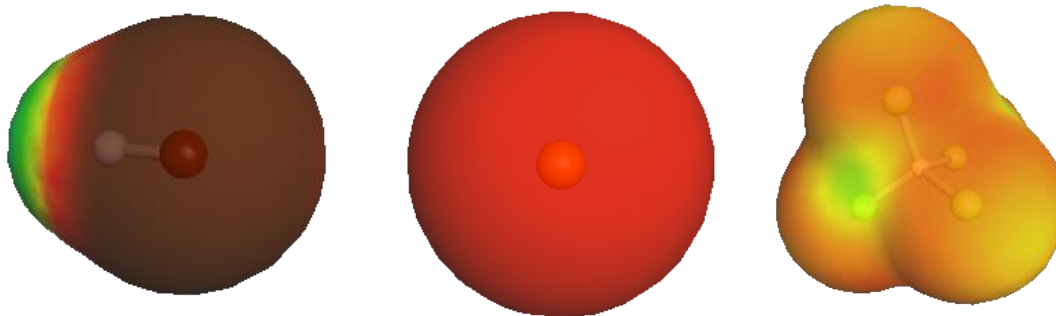


Figure 23. Sigma surfaces of OH⁻, Cl⁻, and BF₄⁻.

As it is shown, OH⁻ anion has a large brown color surface (highest electronegativity), followed by Cl⁻ in red color and finally weakly polarized BF₄⁻ that has partially green and yellow color. Hence, supporting the earlier statement, the further the peak to the right, the larger the sigma value and thus, the more electronegative an anion is. The high electronegativity of OH⁻ anion brings about higher interaction energy and thus interacts better with the water molecules. Meanwhile, BF₄⁻ ion that has its peak close to non-polar region is not really an effective inhibitor anion because of its low polarized charge. This is again proven in Figure 23. Due to the green surface that an BF₄⁻ anion has, it is actually a weak polarized ion and hence shows its peak just right next to the non-polar region in the sigma profile graph. It is thus not a good anion to be tuned as IL inhibitor.

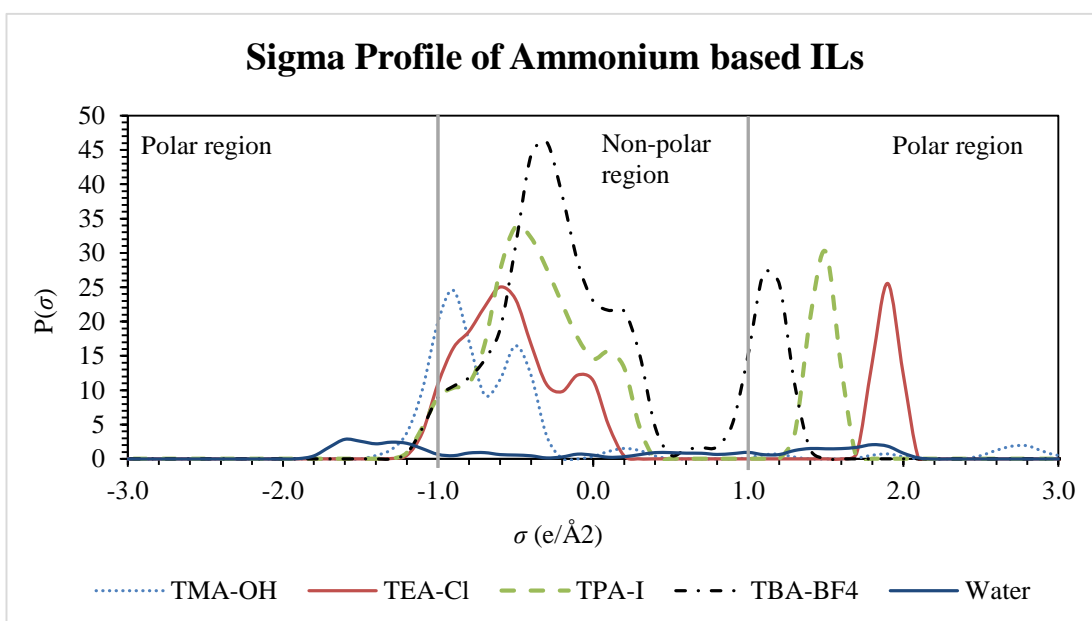


Figure 24. Sigma profile of several ammonium based ILs.

Lastly, the third figure, Figure 24 has selectively displayed the sigma profile graph for four ILs, including TMA-OH, TEA-Cl, TPA-I and TBA-BF₄. The idea of this graph is to showcase several possible combinations of ILs by tuning the cation and anion. Here, it is easily observed that all cations show their peak in the non-polar region. TMA cation shows its peak closest to the polar region and is thus the most suitable cation, due to its higher affinity with water. This could be explained by its short alkyl chain length as compared to others, which makes it more hydrophilic. Meanwhile, all anions lay in the polar region at the right side. The most electronegative anion is definitely OH⁻ ion that has its peak furthest at the right. Due to its highest electronegativity and hence high interaction with water, it serves as the best anion to be used for an inhibitor. Therefore, from the graph, it is identifiable that TMA-OH is the best combination among all. This is followed by TEA-Cl, TPA-Br and finally TBA-BF₄. From this graph, it is inferred that to choose the right anion for hydrate inhibitor, its peak should be located as far as possible at the right side of the graph. This indicates a highly electronegative anion that can bond well with water molecules. Meanwhile, it is reported that most of the ILs cations have their peaks located in the non-polar region. This characteristic causes cations to behave as non-polar molecules that are hydrophobic, and does not interact well with water molecules [49]. Therefore, a cation with lowest hydrophobicity should be chosen to be tuned as hydrate inhibitor, so that it will not hinder interactions between IL and water molecules. This in turn signifies that the most recommendable cation should have its peak closest to the left polar region.

4.2.2 Total Interaction Energies

In section 4.1.2, equation (2) has been developed to describe the relationship between average depression temperature of IL hydrate system and the total interaction energies. It is found out that both cation and anion interaction energy has different effect on IL inhibition ability. High anion interaction energy is preferable, while high cation interaction energy will reduce an IL inhibition ability.

$$\Delta T = 1.758 + 0.0643 E_{INT,C} - 0.00559 E_{INT,A} \quad (2)$$

Using the above correlation, the ability of ammonium based ILs has been predicted through the calculation of average temperature depression. Table 11 below shows the list of ammonium based ILs together with their total interaction energies and predicted inhibition ability measured in terms of average temperature depression.

Table 11. Predicted average temperature depression of AILs.

ILs	$H_{INT,cation}$	$H_{INT,anion}$	$\Delta T_{predicted}$ (°C)
TMA-OH	-14.52	-204.20	1.97
TEA-OH	-18.60	-205.11	1.71
TPA-OH	-27.76	-205.51	1.12
TBA-OH	-37.78	-205.74	0.48
TMA-BF ₄	-16.96	-64.84	1.03
TEA-BF ₄	-20.28	-65.40	0.82
TPA-BF ₄	-28.77	-65.80	0.28
TBA-BF ₄	-38.32	-66.01	-0.34
TMA-Cl	-15.54	-123.28	1.45
TEA-Cl	-19.19	-124.10	1.22
TPA-Cl	-28.12	-124.45	0.65
TBA-Cl	-38.00	-124.64	0.01
TMA-Br	-16.12	-105.40	1.31
TEA-Br	-19.66	-106.10	1.09
TPA-Br	-28.33	-106.43	0.53
TBA-Br	-38.01	-106.60	-0.09
TMA-I	-16.60	-84.49	1.16
TEA-I	-20.06	-85.01	0.94
TPA-I	-28.55	-85.32	0.40
TBA-I	-38.07	-85.50	-0.21

Table 11 generally shows a list of tetraalkylammonium based ILs, which range from cation tetramethylammonium to tetrabutylammonium paired with 5 types of different anions that are hydroxide ion, tetrafluoroborate ion, chloride ion, bromide ion and iodide ion. From this table, it is observed that when anion is fixed, an increase in cation interaction energy, which is caused by the increase in alkyl chain length, will reduce average temperature depression. This again, agrees to the earlier statement which explained that the longer alkyl chain length of cation, the more bulky it is, and thus harder for it to interact with water molecules [21], [51]. This as a result, increases its hydrophobicity, reduces its ability to bond with water and is thus a less effective thermodynamic hydrate inhibitor [36]. In fact, among the five TBA ionic liquids, three of them show negative temperature depression. This is because of the poor combination of bulky cation (TBA) and weak electronegativity anion (Br^- , I^- , BF_4^-), resulting in a super ineffective inhibitor. A negative temperature depression signifies that instead of serving as hydrate inhibitor, they have now become hydrate promoter that favors the formation of hydrate phase.

In terms of effect of anion, we can see that the higher the interaction energy of anion, the higher the average temperature depression. Here, the rank of E_{INT} is as $\text{OH}^- > \text{Cl}^- > \text{Br}^- > \text{I}^- > \text{BF}_4^-$. This resulted in the average temperature depression to follow the same pattern. For instance, looking at tetramethylammonium ILs, inhibition ability rank is as $\text{TMA-OH} > \text{TMA-Cl} > \text{TMA-Br} > \text{TMA-I} > \text{TMA-BF}_4$. Hence, this again proves that the interaction energy provided by anion plays a crucial role in determining its inhibition ability. In addition, this prediction actually agrees well with work reported by Tariq et al [36]. In his review work, he reported that for a methylimidazolium based IL, the order of efficiency follows as such: $\text{C}_2\text{C}_1\text{im-Cl} > \text{C}_2\text{C}_1\text{im-Br} > \text{C}_2\text{C}_1\text{im-I} > \text{C}_2\text{C}_1\text{im-BF}_4$. Regrettably, OH^- ILs are not studied in Tariq's work, yet, the whole ranking ranging from Cl^- to BF_4^- are totally similar to the predicted ranking. This proves that the developed correlation is performing outstandingly in predicting the inhibition ability of ILs. Lastly, from this model, TMA-OH is identified to show the strongest ability as THI, with the highest depression temperature of 1.97°C . This is due to the highly electronegative OH^- anion that bonds well with water molecules and a short alkyl chain length tetramethylammonium cation that does not hinder the IL interaction with water molecules.

CHAPTER 5

CONCLUSION AND RECOMMENDATION

In conclusion, among the four identified fundamental properties, sigma profile and hydrogen bonding energy have been successfully correlated to the inhibition ability of IL. Sigma profile provides a qualitative understanding of each IL in the sense of their affinity towards water molecules. Meanwhile, hydrogen bonding energy, or later upgraded to total interaction energy, has been able to satisfactorily predict out a quantitative value of average temperature depression provided by each IL. This value will then tell us the effectiveness of each IL as thermodynamic hydrate inhibitor. The correlation developed is validated with open literature and is found out to have an average error of 20.49%. Findings however show that this correlation is not suitable to be used for substituted cations, as the introduced functional group such as hydroxyl group will provide extra H-bonding with water molecules. COSMO-RS simulation on the other hand, has been proved to be applicable in computing fundamental properties of IL-hydrate system. Simulation of COSMO-RS in calculating fundamental properties paired with the correlation developed in this work, could now serve as a pre-screening tool of ILs inhibition ability. This helps to narrow down the scope of ILs to be focused during experimental work and thus speed up the rate of potential ILs being tested and applied to industry processes. In the second part of this work, 20 ammonium based ILs have been pre-screened by analysing their sigma profile graph, as well as by predicting their average temperature depression through the developed correlation. Among them, TMA-OH has shown the highest inhibition ability (1.97°C) due to the combination of its short alkyl chain length cation and a highly electronegative OH⁻ anion. It in fact, is predicted to work better than the popularly studied EMIM-Cl, which has only an experimental inhibition ability of 1.22°C.

Due to limited time frame, this work does not include experimental work. In future, experimental work should be conducted: i) to prove the superiority of ammonium based ILs as gas hydrate inhibitors ii) to prove the practicability of correlation and COSMO-RS simulation in predicting properties for gas hydrate state. Lastly, a similar work should be done to develop predictive model for ILs in terms of kinetic hydrate inhibition.

REFERENCES

- [1] B. Li, X. Li, G. Li, Y. Wang, and J. Feng, “Kinetic Behaviors of Methane Hydrate Formation in Porous Media in Different Hydrate Deposits,” *Ind. Eng. Chem. Res.*, 2014.
- [2] K. Nazari, M. R. Moradi, and a. N. Ahmadi, “Kinetic Modeling of Methane Hydrate Formation in the Presence of Low-Dosage Water-Soluble Ionic Liquids,” *Chem. Eng. Technol.*, vol. 36, no. 11, pp. 1915–1923, 2013.
- [3] V. R. Avula, R. L. Gardas, and J. S. Sangwai, “An efficient model for the prediction of CO₂ hydrate phase stability conditions in the presence of inhibitors and their mixtures,” *J. Chem. Thermodyn.*, vol. 85, pp. 163–170, Jun. 2015.
- [4] K.-S. Kim, J. W. Kang, and S.-P. Kang, “Tuning ionic liquids for hydrate inhibition,” *Chem. Commun. (Camb.)*, vol. 47, no. 22, pp. 6341–6343, 2011.
- [5] K. M. Sabil, O. Nashed, B. Lal, L. Ismail, and A. Japper-Jaafar, “Experimental investigation on the dissociation conditions of methane hydrate in the presence of imidazolium-based ionic liquids,” *J. Chem. Thermodyn.*, vol. 84, pp. 7–13, 2015.
- [6] H. Zeng, L. D. Wilson, V. K. Walker, and J. a. Ripmeester, “Effect of antifreeze proteins on the nucleation, growth, and the memory effect during tetrahydrofuran clathrate hydrate formation,” *J. Am. Chem. Soc.*, vol. 128, no. 9, pp. 2844–2850, 2006.
- [7] M. A. Kelland, “History of the Development of Low Dosage Hydrate Inhibitors,” *Energy & Fuels*, vol. 20, no. 3, pp. 825–847, May 2006.
- [8] S. Y. Hong, J. Il Lim, J. H. Kim, and J. D. Lee, “Kinetic studies on methane hydrate formation in the presence of kinetic inhibitor via in situ Raman spectroscopy,” *Energy and Fuels*, vol. 26, no. 11, pp. 7045–7050, 2012.
- [9] C. Xiao and H. Adidharma, “Dual function inhibitors for methane hydrate,” *Chem. Eng. Sci.*, vol. 64, no. 7, pp. 1522–1527, 2009.
- [10] C. Xiao, N. Wibisono, and H. Adidharma, “Dialkylimidazolium halide ionic liquids as dual function inhibitors for methane hydrate,” *Chem. Eng. Sci.*, vol. 65, no. 10, pp. 3080–3087, 2010.
- [11] A. Klamt, *COSMO-RS: From Quantum Chemistry to Fluid Phase Thermodynamics and Drug Design*, 1st ed. Amsterdam: Elsevier, 2005.
- [12] I. Khan, K. A. Kurnia, T. E. Sintra, J. A. Saraiva, S. P. Pinho, and J. A. P. Coutinho, “Assessing the activity coefficients of water in cholinium-based ionic liquids: Experimental measurements and COSMO-RS modeling,” *Fluid Phase Equilib.*, vol. 361, pp. 16–22, Jan. 2014.

- [13] R. Franke, B. Hannebauer, and S. Jung, “Accurate pre-calculation of limiting activity coefficients by COSMO-RS with molecular-class based parameterization,” *Fluid Phase Equilib.*, vol. 340, pp. 11–14, Feb. 2013.
- [14] M. Diedenhofen and A. Klamt, “COSMO-RS as a tool for property prediction of IL mixtures—A review,” *Fluid Phase Equilib.*, vol. 294, no. 1–2, pp. 31–38, Jul. 2010.
- [15] M. Diedenhofen, F. Eckert, A. Klamt, C. Gmbh, C. Kg, B. Strasse, and D.-Leverkusen, “Compounds in Ionic Liquids Using COSMO-RS †,” *Engineering*, no. 1, pp. 475–479, 2003.
- [16] M. Grabda, M. Panigrahi, S. Oleszek, D. Kozak, F. Eckert, E. Shibata, and T. Nakamura, “COSMO-RS screening for efficient ionic liquid extraction solvents for NdCl₃ and DyCl₃,” *Fluid Phase Equilib.*, vol. 383, pp. 134–143, 2014.
- [17] M. Diedenhofen, F. Eckert, and A. Klamt, “Prediction of infinite dilution activity coefficients of organic compounds in ionic liquids using COSMO-RS,” *J. Chem. ...*, 2003.
- [18] Q. Chen, Y. Yu, P. Zeng, W. Yang, Q. Liang, X. Peng, Y. Liu, and Y. Hu, “Effect of 1-butyl-3-methylimidazolium tetrafluoroborate on the formation rate of CO₂ hydrate,” *J. Nat. Gas Chem.*, vol. 17, no. 3, pp. 264–267, Sep. 2008.
- [19] A. R. Richard and H. Adidharma, “The performance of ionic liquids and their mixtures in inhibiting methane hydrate formation,” *Chem. Eng. Sci.*, vol. 87, pp. 270–276, 2013.
- [20] X. Sen Li, Y. J. Liu, Z. Y. Zeng, Z. Y. Chen, G. Li, and H. J. Wu, “Equilibrium hydrate formation conditions for the mixtures of methane + ionic liquids + water,” *J. Chem. Eng. Data*, vol. 56, no. 1, pp. 119–123, 2011.
- [21] L. Keshavarz, J. Javanmardi, A. Eslamimanesh, and A. H. Mohammadi, “Experimental measurement and thermodynamic modeling of methane hydrate dissociation conditions in the presence of aqueous solution of ionic liquid,” *Fluid Phase Equilib.*, vol. 354, pp. 312–318, 2013.
- [22] A. Klamt, “Conductor-like Screening Model for Real Solvents: A New Approach to the Quantitative Calculation of Solvation Phenomena,” *J. Phys. Chem.*, vol. 99, no. 7, pp. 2224–2235, 1995.
- [23] K. a. Kurnia, S. P. Pinho, and J. a P. Coutinho, “Evaluation of the conductor-like screening model for real solvents for the prediction of the water activity coefficient at infinite dilution in ionic liquids,” *Ind. Eng. Chem. Res.*, vol. 53, no. 31, pp. 12466–12475, 2014.
- [24] N. Calvar, I. Dom ínguez, E. Gómez, J. Palomar, and Á. Dom ínguez, “Evaluation of ionic liquids as solvent for aromatic extraction: Experimental,

- correlation and COSMO-RS predictions,” *J. Chem. Thermodyn.*, vol. 67, pp. 5–12, 2013.
- [25] M. G. Freire, S. P. M. Ventura, L. M. N. B. F. Santos, I. M. Marrucho, and J. A. P. Coutinho, “Evaluation of COSMO-RS for the prediction of LLE and VLE of water and ionic liquids binary systems,” *Fluid Phase Equilib.*, vol. 268, no. 1–2, pp. 74–84, Jun. 2008.
- [26] I. Domínguez, E. J. González, J. Palomar, and Á. Domínguez, “Phase behavior of ternary mixtures {aliphatic hydrocarbon + aromatic hydrocarbon + ionic liquid}: Experimental LLE data and their modeling by COSMO-RS,” *J. Chem. Thermodyn.*, vol. 77, pp. 222–229, 2014.
- [27] R. Anantharaj and T. Banerjee, “COSMO-RS-Based Screening of Ionic Liquids as Green Solvents in Denitrification Studies,” *Ind. Eng. Chem. Res.*, vol. 49, no. 18, pp. 8705–8725, Sep. 2010.
- [28] M. Grabda, S. Oleszek, M. Panigrahi, D. Kozak, F. Eckert, E. Shibata, and T. Nakamura, “Theoretical selection of most effective ionic liquids for liquid–liquid extraction of NdF₃,” *Comput. Theor. Chem.*, vol. 1061, pp. 72–79, Jun. 2015.
- [29] K. Kurnia and M. Mutalib, “Selection of ILs for Separation of Benzene from n-Hexane Using COSMO-RS. A Quantum Chemical Approach,” *Key Eng. ...*, 2013.
- [30] J. Palomar, V. R. Ferro, J. S. Torrecilla, and F. Rodríguez, “Density and molar volume predictions using COSMO-RS for ionic liquids. An approach to solvent design,” *Ind. Eng. Chem. Res.*, vol. 46, no. 18, pp. 6041–6048, 2007.
- [31] K. Z. Sumon and A. Henni, “Ionic liquids for CO₂ capture using COSMO-RS: Effect of structure, properties and molecular interactions on solubility and selectivity,” *Fluid Phase Equilib.*, vol. 310, no. 1–2, pp. 39–55, Nov. 2011.
- [32] S. Pilli, K. Mohanty, and T. Banerjee, “Extraction of Phthalic Acid from Aqueous Solution by Using Ionic Liquids: A Quantum Chemical Approach,” *Int. J. Thermodyn.*, vol. 17, no. 1, pp. 42–51, 2014.
- [33] K. Machanová, J. Troncoso, J. Jacquemin, and M. Bendová, “Excess molar volumes and excess molar enthalpies in binary systems N-alkyl-triethylammonium bis(trifluoromethylsulfonyl)imide+methanol,” *Fluid Phase Equilib.*, vol. 363, pp. 156–166, 2014.
- [34] E. Mullins, R. Oldland, and Y. Liu, “Sigma-profile database for using COSMO-based thermodynamic methods,” *Ind. ...*, 2006.
- [35] S. J. French, *Nature of the Chemical Bond*, Second. New York: Cornell University Press, 1948.

- [36] M. Tariq, D. Rooney, E. Othman, S. Aparicio, M. Atilhan, and M. Khraisheh, "Gas Hydrate Inhibition: A Review of the Role of Ionic Liquids," *Ind. Eng. Chem. Res.*, vol. 53, no. 46, pp. 17855–17868, Nov. 2014.
- [37] A. F. M. Cláudio, L. Swift, J. P. Hallett, T. Welton, J. a P. Coutinho, and M. G. Freire, "Extended scale for the hydrogen-bond basicity of ionic liquids.," *Phys. Chem. Chem. Phys.*, vol. 16, no. 14, pp. 6593–601, 2014.
- [38] T. Zhou, L. Chen, Y. Ye, L. Chen, Z. Qi, H. Freund, and K. Sundmacher, "An Overview of Mutual Solubility of Ionic Liquids and Water Predicted by COSMO-RS," *Ind. Eng. Chem. Res.*, vol. 51, no. 17, pp. 6256–6264, May 2012.
- [39] S. Omar, J. Lemus, E. Ruiz, V. R. Ferro, J. Ortega, and J. Palomar, "Ionic liquid mixtures - An analysis of their mutual miscibility," *J. Phys. Chem. B*, vol. 118, no. 9, pp. 2442–2450, 2014.
- [40] R. P. Swatoski, S. K. Spear, J. D. Holbrey, and R. D. Rogers, "Dissolution of cellulose [correction of cellose] with ionic liquids.," *J. Am. Chem. Soc.*, vol. 124, no. 18, pp. 4974–4975, 2002.
- [41] Y. A. Kholod, G. Gryn'ova, L. Gorb, F. C. Hill, and J. Leszczynski, "Evaluation of the dependence of aqueous solubility of nitro compounds on temperature and salinity: a COSMO-RS simulation.," *Chemosphere*, vol. 83, no. 3, pp. 287–94, Apr. 2011.
- [42] K. Machanová, J. Jacquemin, Z. Wagner, and M. Bendová, "Mutual Solubilities of Ammonium-Based Ionic Liquids with Water and with Water/Methanol Mixture," *Procedia Eng.*, vol. 42, pp. 1229–1241, 2012.
- [43] M. Zare, A. Haghtalab, A. N. Ahmadi, and K. Nazari, "Experiment and thermodynamic modeling of methane hydrate equilibria in the presence of aqueous imidazolium-based ionic liquid solutions using electrolyte cubic square well equation of state," *Fluid Phase Equilib.*, vol. 341, no. October, pp. 61–69, 2013.
- [44] A. Schäfer, C. Huber, and R. Ahlrichs, "Fully optimized contracted Gaussian basis sets of triple zeta valence quality for atoms Li to Kr," *J. Chem. Phys.*, vol. 100, no. 8, pp. 5829–5835, 1994.
- [45] S. Z. S. Jaapar, Y. Iwai, and N. A. Morad, "Effect of Co-Solvent on the Solubility of Ginger Bioactive Compounds in Water Using COSMO-RS Calculations," *Appl. Mech. Mater.*, vol. 624, no. June, pp. 174–178, 2014.
- [46] T. Ingram, T. Gerlach, T. Mehling, and I. Smirnova, "Extension of COSMO-RS for monoatomic electrolytes: Modeling of liquid–liquid equilibria in presence of salts," *Fluid Phase Equilib.*, vol. 314, pp. 29–37, Jan. 2012.
- [47] K. a. Kurnia and J. a P. Coutinho, "Overview of the excess enthalpies of the binary mixtures composed of molecular solvents and ionic liquids and their

- modeling using COSMO-RS,” *Ind. Eng. Chem. Res.*, vol. 52, no. 38, pp. 13862–13874, 2013.
- [48] X. Peng, Y. Hu, Y. Liu, C. Jin, and H. Lin, “Separation of ionic liquids from dilute aqueous solutions using the method based on CO₂ hydrates,” *J. Nat. Gas Chem.*, vol. 19, no. 1, pp. 81–85, 2010.
- [49] A. Klamt, “COSMO-RS for aqueous solvation and interfaces,” *Fluid Phase Equilib.*, 2015.
- [50] G. Gonfa, M. A. Bustam, A. M. Sharif, N. Mohamad, and S. Ullah, “Tuning Ionic liquids for Natural Gas Dehydration Using COSMO-RS Methodology,” *J. Nat. Gas Sci. Eng.*, Sep. 2015.
- [51] V. R. Avula, R. L. Gardas, and J. S. Sangwai, “An improved model for the phase equilibrium of methane hydrate inhibition in the presence of ionic liquids,” *Fluid Phase Equilib.*, vol. 382, pp. 187–196, 2014.
- [52] B. Partoon, N. M. S. Wong, K. M. Sabil, K. Nasrifar, and M. R. Ahmad, “A study on thermodynamics effect of [EMIM]-Cl and [OH-C2MIM]-Cl on methane hydrate equilibrium line,” *Fluid Phase Equilib.*, vol. 337, pp. 26–31, Jan. 2013.
- [53] K. Kim and S.-P. Kang, “Investigation of Pyrrolidinium- and Morpholinium-Based Ionic Liquids Into Kinetic Hydrate Inhibitors on Structure I Methane Hydrate,” *7th International Conference Gas Hydrates 2011*, no. Icgh, p. 6, 2011.